



THE UNIVERSITY *of* EDINBURGH

Edinburgh Research Explorer

Nonlinear viscoelastic characterization of bovine trabecular bone

Citation for published version:

Manda, K, Wallace, R, Xie, S, Levrero-Florencio, F & Pankaj, P 2017, 'Nonlinear viscoelastic characterization of bovine trabecular bone' *Biomechanics and Modeling in Mechanobiology*, vol. 16, no. 1, pp. 173-189; 191-195. DOI: 10.1007/s10237-016-0809-y

Digital Object Identifier (DOI):

[10.1007/s10237-016-0809-y](https://doi.org/10.1007/s10237-016-0809-y)

Link:

[Link to publication record in Edinburgh Research Explorer](#)

Document Version:

Peer reviewed version

Published In:

Biomechanics and Modeling in Mechanobiology

General rights

Copyright for the publications made accessible via the Edinburgh Research Explorer is retained by the author(s) and / or other copyright owners and it is a condition of accessing these publications that users recognise and abide by the legal requirements associated with these rights.

Take down policy

The University of Edinburgh has made every reasonable effort to ensure that Edinburgh Research Explorer content complies with UK legislation. If you believe that the public display of this file breaches copyright please contact openaccess@ed.ac.uk providing details, and we will remove access to the work immediately and investigate your claim.



1 **Nonlinear viscoelastic characterization of bovine trabecular**
2 **bone**

3 **Krishnagoud Manda · Robert J. Wallace · Shuqiao**
4 **Xie · Francesc Levrero-Florencio · Pankaj Pankaj**

5
6 the date of receipt and acceptance should be inserted later

7 **Abstract** The time-independent elastic properties of trabecular bone have been extensively
8 investigated and several stiffness-density relations have been proposed. Although it is recog-
9 nised that trabecular bone exhibits time-dependent mechanical behaviour, a property of vis-
10 coelastic materials, the characterization of this behaviour has received limited attention. The
11 objective of the present study was to investigate the time-dependent behaviour of bovine
12 trabecular bone through a series of compressive creep-recovery experiments and to iden-
13 tify its nonlinear constitutive viscoelastic material parameters. Uniaxial compressive creep
14 and recovery experiments at multiple loads were performed on cylindrical bovine trabecular
15 bone samples ($n = 19$). Creep response was found to be significant and always comprised
16 of recoverable and irrecoverable strains, even at low stress/strain levels. This response was
17 also found to vary nonlinearly with applied stress. A systematic methodology was developed

Krishnagoud Manda (✉) · Shuqiao Xie · Francesc Levrero-Florencio · Pankaj Pankaj

School of Engineering, The University of Edinburgh, The King's Buildings, Edinburgh, EH9 3DW, UK

E-mail: k.manda@ed.ac.uk

Robert J. Wallace

Department of Orthopaedics, The University of Edinburgh, Chancellors building, Edinburgh, EH16 4SB, UK

18 to separate recoverable (nonlinear viscoelastic) and irrecoverable (permanent) strains from
19 the total experimental strain response. We found that Schapery's nonlinear viscoelastic con-
20 stitutive model describes the viscoelastic response of the trabecular bone, and parameters
21 associated with this model were estimated from the multiple load creep-recovery (MLCR)
22 experiments. Nonlinear viscoelastic recovery compliance was found to have a decreasing
23 and then increasing trend with increasing stress level, indicating possible stiffening and soft-
24 ening behaviour of trabecular bone due to creep. The obtained parameters from MLCR tests,
25 expressed as second order polynomial functions of stress, showed a similar trend for all the
26 samples, and also demonstrate stiffening-softening behaviour with increasing stress.

27 **Keywords** Creep · recovery · nonlinear viscoelasticity · recoverable and irrecoverable
28 strains · trabecular bone · Schapery model

29 **1 Introduction**

30 Trabecular bone is an open porous composite cellular solid material from an engineering
31 perspective. The apparent level mechanical properties of this cellular material depend on
32 its heterogeneous microstructure, which varies with age, disease, gender and anatomical site
33 being considered (Keaveny et al, 2001). Bone is known to become more porous with age and
34 due to diseases such as osteoporosis (Rachner et al, 2011). Trabecular bone is anisotropic
35 and principal trabecular orientations vary with anatomical site; it is also recognised that its
36 anisotropic character becomes pronounced with age (Singh et al, 1970). The density of this
37 cellular solid has been related to its time-independent elastic stiffness in a number of studies
38 (Currey, 1986; Morgan et al, 2003) and these relations are frequently used in computational
39 models of bone and bone-implant systems (Goffin et al, 2013). It has also been recognised
40 that the response of bone to mechanical loads is, in reality, time-dependent (Schoenfeld et al,

41 1974; Zilch et al, 1980). The study of time-dependent behaviour is of interest in a number of
42 contexts: loosening of orthopaedic implants; non traumatic fractures due to prolonged load
43 over time; viscoelastic compatibility of synthetic bone substitutes; and energy absorption
44 during dynamic loads (Norman et al, 2006; Pollintine et al, 2009; Phillips et al, 2006; Linde
45 et al, 1989).

46 The time-dependent mechanical behaviour of the trabecular bone has been experimen-
47 tally investigated via relaxation tests (Schoenfeld et al, 1974; Zilch et al, 1980; Deligianni
48 et al, 1994; Bredbenner and Davy, 2006; Quaglini et al, 2009), creep tests (Bowman et al,
49 1994, 1998; Yamamoto et al, 2006; Manda et al, 2016), and dynamic mechanical tests
50 (Guedes et al, 2006; Kim et al, 2012, 2013). Yamamoto et al (2006) reported that substantial
51 amount of creep develops in the trabecular bone even at smaller load levels corresponding to
52 physiological activities. It has also been found that the time-dependent response is not linear
53 and varies with the applied stress/strain levels (Bowman et al, 1998; Yamamoto et al, 2006;
54 Quaglini et al, 2009), i.e. it cannot be modelled using linear viscoelasticity. However, none
55 of the above studies quantified the nonlinearity in the time-dependent response of the tra-
56 becular bone. Characterizing this nonlinearity in the time-dependent behaviour at apparent
57 level is important from both clinical and engineering perspectives. Such characterization can
58 provide: insights into the mechanisms contributing to the creep behaviour of the trabecular
59 bone; improve predictions from finite element modelling of bone and bone-implant systems;
60 and help understand osteoporotic fractures.

61 Many constitutive equations have been developed for characterizing the nonlinear vis-
62 coelastic materials, from single integral (Knauss and Emri, 1981; Schapery, 1969; Chris-
63 tensen, 1980) to multiple integral formulations, see e.g. Findley et al (1976). The single
64 integral representations have been the most widely applied theories for different viscoelastic
65 materials and are relatively easy to implement in a numerical scheme. Previous studies have

66 developed methodologies to determine the nonlinear viscoelastic parameters based on sin-
67 gle integral formulations for materials with power law time dependence (Lou and Schapery,
68 1971) and with Prony series time-dependence (Nordin and Varna, 2005; Huang et al, 2011).
69 Both creep data during plateau loading and strain recovery data after unloading in a creep-
70 recovery test at different load levels are required for this analysis. Most of these formulations
71 have been used for materials like asphalt concrete and polymers, and the samples were per-
72 mitted to fully recover between creep-recovery tests at different load levels. However, it is
73 not known how long trabecular bone takes to recover fully between the tests (Yamamoto
74 et al, 2006; Kim et al, 2012; Pollintine et al, 2009). Therefore it is necessary to develop a
75 methodology that takes into account any residual strains and permits continuous application
76 of loading and unloading phases at different load levels without the need for resting the
77 sample between the loading cycles.

78 Therefore, the primary objectives of the study were three-fold. First, to experimentally
79 measure the time-dependent behaviour of trabecular bone through uniaxial compressive
80 multiple load creep-recovery (MLCR) experiments. Second, to develop a systemic method-
81 ology to estimate the associated material parameters from the MLCR tests. Third, to quantify
82 the nonlinearity associated with varying stress levels using the obtained parameters.

83 **2 Materials and methods**

84 **2.1 Sample preparation and μ CT imaging**

85 Fresh proximal bovine femora, female, under 30 months old when killed, were obtained
86 from a local abattoir and were stored at -20 °C until utilized. The bones were allowed to
87 thaw to room temperature before the femoral heads and trochanters were removed using
88 a hacksaw. Transmission radiographs were then taken to identify the principal direction of

89 trabeculae, and 19 cores (15 from three femoral heads and 4 from two trochanters) were
90 extracted using a diamond core drill bit (Starlite, Rosemont, USA) and marrow was kept
91 intact in all the samples to mimic the realistic situation of bone as closely as possible. The
92 heads and trochanters were kept hydrated while drilling in a custom made holding clamp to
93 mitigate temperature damage. Once extracted, the cores were examined for the presence of a
94 growth plate, and if found this was removed during sample preparation. A low speed rotating
95 saw (Buehler, Germany) was used to create parallel sections. The cylindrical bone samples
96 in total $n = 19$ were of diameter 10.6 ± 0.1 mm and mean height of 25.0 ± 2.7 mm. Brass
97 end-caps were glued to each end of the sample using bone cement (Simplex, Stryker, UK) to
98 minimize end-artefacts during compression testing (Keaveny et al, 1997). Effective length
99 (22.1 ± 2.6 mm) of each specimen was calculated as the length of the sample between the
100 end-caps plus half the length of the sample embedded within the end-caps (Keaveny et al,
101 1997), and this effective length was used in calculating average strains.

102 Before mechanical testing high resolution microcomputed tomography (μ CT) scans
103 were taken of each sample using a Skyscan 1172 μ CT scanner (Bruker microCT, Kontich,
104 Belgium). The following scan parameters were used: voxel resolution $17.22 \mu\text{m}$, source
105 voltage 100 kV, current $100 \mu\text{A}$, exposure 1771 ms with a 0.5 mm aluminium filter between
106 the x-ray source and the specimen. Image quality was improved by using 2 frame averag-
107 ing. The images were reconstructed with no further reduction in resolution using Skyscan
108 proprietary software, nRecon V1.6.9.4 (Bruker microCT, Kontich, Belgium). Morphometric
109 analysis was performed using CTAn software (Bruker microCT, Kontich, Belgium), and by
110 considering the whole volume within each sample the ratio of bone volume to total volume
111 (BV/TV) was evaluated along with other microarchitectural indices: trabecular thickness
112 (Tb.Th), trabecular number (Tb.N), trabecular separation (Tb.Sp) and structure model in-
113 dex (SMI). Homogeneity analysis was performed on each sample by evaluating the above

114 microarchitectural indices in sub-volumes of four $5 \times 5 \times 5$ mm cubes along the length of
115 each sample. Intra-specimen variations of these indices across each sample were found to
116 be less than $\pm 4\%$ with respect to the values when whole volume was considered indicating
117 fairly homogeneous nature and uniform bone quality of each sample. A water bath filled
118 with phosphate-buffered saline (PBS) was used around each sample to keep it hydrated at
119 all times during imaging and through all phases of mechanical testing.

120 2.2 Creep-recovery experiments

121 Following μ CT scanning, each sample was preconditioned by applying 0.1% apparent strain
122 for ten cycles (Bowman et al, 1994) and was then allowed to recover for 30 minutes prior to
123 the main mechanical testing. The compressive multiple load creep-recovery (MLCR) exper-
124 iments as shown in Fig. 1 were conducted on 19 trabecular bone samples using Zwick ma-
125 terial testing machine (Zwick Roell, Herefordshire, UK). The trabecular bone macroscop-
126 ically yields below 0.8% strains in compression (Kopperdahl and Keaveny, 1998; Morgan
127 et al, 2001) in an isotropic manner in strain space (Leverero-Florencio et al, 2016). There-
128 fore, we chose the static strains of 0.2%, 0.4%, 0.6%, 0.8%, 1.0%, 1.5%, 2.0% and 2.5% in
129 cycles I-VIII, respectively, to measure the time-dependent behaviour at pre and post yield
130 regime. These target strains were specified to the Zwick machine in the MLCR tests on each
131 sample which in turn applied the force as a ramp at a strain rate of 0.01 s^{-1} , and when the
132 targeted static strain was reached, a constant load corresponding to this strain was automati-
133 cally maintained by the machine for 200 s. Each loading step was followed by an unloading
134 step (again at a strain rate of 0.01 s^{-1}) to almost zero (2 N) force, which was maintained for
135 600 s (see upper part of Fig. 1). This small load of 2 N was to ensure that end-caps remained
136 in contact with the load applicator. The creep deformation was recorded during the loading

137 phase of 200 s and also during the strain recovery (unloading phase) of 600 s for each cycle
 138 throughout the experiment for each sample (lower part of Fig. 1). All the tests were load
 139 controlled. In our pilot studies, we observed that the creep rate (slope of the creep vs time
 140 curve) becomes constant in less than 200 s during the loading phase (at load levels of inter-
 141 est). Similarly in the recovery phase the recovery curves were found to reach a plateau in
 142 less than 600 s. Hence, we chose the creep time as 200 s and recovery time as 600 s for all
 143 samples in all cycles.

144 These multiple plateau loads corresponding to above mentioned static strains were con-
 145 verted to stresses by dividing them with cross sectional area of each sample. The experi-
 146 ments were stopped if the tertiary creep or failure occurred during the loading phase at any
 147 stress level. The tertiary creep or failure was defined as response where creep strain acceler-
 148 ates rapidly and increases beyond 5.0%. In the following sections we use the term ‘load’ in
 149 Newtons and ‘stress’ in MPa interchangeably, and also a term ‘applied static strain’ which
 150 indicates the plateau loads/stresses corresponding to static strains of 0.2%, 0.4%, 0.6%,
 151 0.8%, 1.0%, 1.5%, 2.0% and 2.5% in the loading cycles I, II, III, IV, V, VI, VII and VIII,
 152 respectively.

153 2.3 Material model

154 The time-dependent strain response ($\epsilon_{tot}(t)$) of trabecular bone to an applied load is given
 155 by

$$156 \quad \epsilon_{tot}(t) = \epsilon_{nve}(t) + \epsilon_{irrec}(t) \quad (1)$$

157 where $\epsilon_{irrec}(t)$ is the irrecoverable strain response and $\epsilon_{nve}(t)$ is the recoverable nonlinear
 158 viscoelastic strain. For linear viscoelastic materials $\epsilon_{nve}(t) = \epsilon_{ve}(t)$ and Boltzmann super-
 159 position integral, can be used to represent the stress-strain relations (Findley et al, 1976), is

160 given by

$$161 \quad \varepsilon_{ve}(t) = \int_0^t D(t-\tau) \frac{d\sigma}{d\tau} \tau \quad (2)$$

162 or, equivalently

$$163 \quad \varepsilon_{ve}(t) = D_0\sigma + \int_0^t \Delta D(t-\tau) \frac{d\sigma}{d\tau} \tau \quad (3)$$

164 where σ is an arbitrary stress input, $D(t) = D_0 + \Delta D(t)$ is the total creep compliance, D_0
 165 is instantaneous compliance that describes the elastic response at time $t = 0$ and $\Delta D(t)$ is
 166 the transient creep compliance that evolves with time. In an ideal creep-recovery test, the
 167 plateau stress σ is applied at time $t = 0$ and removed at $t = t_a$ (see the first cycle in Fig. 1).

168 By substituting this step input of stress σ into Eq. 3, the resulting creep strain response (ε_{cr})
 169 during loading phase, $0 < t < t_a$, in a typical creep-recovery test is obtained as

$$170 \quad \varepsilon_{cr}(t) = D_0\sigma + \Delta D(t)\sigma + \varepsilon_{irrec}(t) \quad (4)$$

171 and the strain response during recovery period (ε_{re}), $t > t_a$, is given by

$$172 \quad \begin{aligned} \varepsilon_{re}(t) &= \varepsilon_{cr}(t) - \varepsilon_{cr}(t-t_a) \\ &= [\Delta D(t) - \Delta D(t-t_a)]\sigma + \varepsilon_{irrec}(t_a) \end{aligned} \quad (5)$$

173 It is important to note that it is not possible to perform, in practice, ideal creep-recovery
 174 experiments with instantaneous load application at $t = 0$. In this study, the load application
 175 in MLCR tests was a finite ramp with the strain rate of 0.01 s^{-1} . We assumed that this strain
 176 rate is sufficiently fast to be treated as instantaneous for the range of strains considered in
 177 this study; it was, therefore, assumed that it has negligible influence on the results.

178 Our preliminary experimental analysis revealed that the recoverable behaviour is not
 179 linear and is dependent on the applied stress. Also previous studies (Yamamoto et al, 2006;
 180 Quaglini et al, 2009) have recognised that the time-dependent behaviour of the trabecular
 181 bone is not linear and varies with the applied stress/strain. In order to capture this nonlinear-
 182 ity, the stress-dependent nonlinear viscoelastic models were considered in this study.

183 Several general constitutive models have been proposed to describe the behaviour of
 184 nonlinear viscoelastic materials (Schapery, 1969; Christensen, 1980; Knauss and Emri,
 185 1981). The thermodynamics based theory using single integral nonlinear viscoelasticity de-
 186 veloped by Schapery (1969, 1997), which utilizes the same structure as the linear integral
 187 model, has been shown to be a convenient formulation (Smart and Williams, 1972). Also,
 188 Dillard et al (1987) compared the Schapery's model to several other nonlinear viscoelas-
 189 tic formulations and showed that Schapery's model produces most accurate results for both
 190 given stress or strain inputs. It has also been shown that this model is adaptable to many
 191 other nonlinear viscoelastic materials, like asphalt concrete (Huang et al, 2011), polymers
 192 (Lai and Bakker, 1995), and ligaments (Provenzano et al, 2002). It was, therefore thought
 193 to be appropriate for modelling trabecular bone in this study. The nonlinear constitutive pa-
 194 rameters in the Schapery's model conveniently describe the nonlinearities based on stress.

195 The nonlinear viscoelastic model proposed by Schapery (1969) is given by

$$196 \quad \varepsilon_{nve}(t) = g_0 D_0 \sigma + g_1 \int_0^t \Delta D(\psi^t - \psi^\tau) \frac{d(g_2 \sigma)}{d\tau} d\tau \quad (6)$$

197 where g_0 , g_1 , g_2 and a_σ are stress dependent nonlinear viscoelastic (VE) parameters. The
 198 parameter g_0 is a nonlinear instantaneous compliance parameter that scales the reduction
 199 or increase in instantaneous elastic compliance. Transient nonlinear parameter g_1 measures
 200 the nonlinearity effect in the transient compliance, and the parameter g_2 describes the effect
 201 of the loading rate on the transient creep response as well, and ψ^t , called, reduced time, is
 202 given by

$$203 \quad \psi^t = \int_0^t \frac{d\tau'}{a_\sigma(\tau') a_T(\tau') a_e(\tau')} \quad (7)$$

204 where a_σ , a_T and a_e are stress, temperature and other environment time-shift factors, re-
 205 spectively. In this work, the effects of temperature and other environment variables are not
 206 considered and therefore $a_T = a_e = 1$. For the linear viscoelastic materials, the parameters

207 $g_0 = g_1 = g_2 = a_\sigma = 1$, such that the Eq. 6 reduces to the Boltzmann superposition integral
 208 of Eq. 3. The transient compliance in Eq. 6 is represented by Prony series as

$$209 \quad \Delta D(\psi^t) = \sum_{n=1}^{N_{pr}} D_n [1 - \exp(-\lambda_n \psi^t)] \quad (8)$$

210 where N_{pr} is number of Prony series parameters, D_n is n th coefficient of the Prony series
 211 associated with the reciprocal of n th retardation time, λ_n . Similar to the Eqs. 4 and 5, the
 212 strain responses during loading and recovery phases in a typical creep-recovery test are given
 213 by

$$214 \quad \varepsilon_{cr}(t) = g_0 D_0 \sigma + g_1 g_2 \Delta D\left(\frac{t}{a_\sigma}\right) \sigma + \varepsilon_{irrec}(t) \quad (9)$$

215 and

$$216 \quad \varepsilon_{re}(t) = \left[g_2 \sigma \Delta D\left(\frac{t}{a_\sigma}\right) - g_2 \sigma \Delta D\left(\frac{t-t_a}{a_\sigma}\right) \right] + \varepsilon_{irrec}(t_a) \quad (10)$$

217 and the reduced time in Eq. 7 becomes $\psi^t = t/a_\sigma$.

218 2.4 Evaluation of model parameters

219 After selecting Schapery's constitutive theory, the numerical values of its associated param-
 220 eters were obtained in a systematic manner from the MLCR experimental data. Most of the
 221 approaches that have been suggested previously (Lai and Bakker, 1995; Huang et al, 2011)
 222 relied on independent creep-recovery tests in which the samples were allowed to recover
 223 fully between the tests at different load levels. In this study the experiments were performed
 224 continuously at multiple stress levels with loading and unloading phases. Consequently our
 225 methodology was required to account for residual strains from the previous loading cycles
 226 when evaluating the response of the following loading cycle. A schematic depiction of creep
 227 and recovery curves, during loading and unloading phases respectively, at multiple stress
 228 levels is shown in Fig. 1.

229 The components of total strain during the loading and the recovery phases in the first
230 cycle are given by

$$231 \quad \varepsilon_{cr}^I(t) = \left[g_0^I D_0 \sigma^I + g_1^I g_2^I \sigma^I \Delta D \left(\frac{t}{a_\sigma^I} \right) \right] + \varepsilon_{irrec}^I(t) \quad (11)$$

232 and

$$233 \quad \varepsilon_{re}^I(t) = \left[g_2^I \sigma^I \Delta D \left(\frac{t}{a_\sigma^I} \right) - g_2^I \sigma^I \Delta D \left(\frac{t-t_a}{a_\sigma^I} \right) \right] + \varepsilon_{irrec}^I(t_a) \quad (12)$$

234 where superscripts denote the loading cycle number, and subscripts to the time variable t are
235 different time points in the MLCR test as shown in Fig. 1.

236 First step in the analysis procedure is to obtain the Prony series coefficients associated
237 with linear viscoelastic response. It was assumed that the trabecular bone behaves in a linear
238 viscoelastic manner until the first loading cycle (or at a lowest stress level corresponding to
239 0.2% of static strain) for each sample. Hence, the corresponding nonlinear VE parameters
240 $g_0^I = g_1^I = g_2^I = a_\sigma^I = 1$ for the first loading cycle. The irrecoverable strain, in the first cy-
241 cle, is constant once the load is removed at $t = t_a$, and therefore, by taking the difference
242 between Eq. 11 at $t = t_a$ and Eq. 12 it is possible to eliminate the irrecoverable strain and
243 the remainder gives purely recoverable (viscoelastic) response. Therefore, the viscoelastic
244 recovery strain $\Delta \varepsilon_{re1}^I$ between t_a and t_b in the first loading cycle is given by

$$\begin{aligned} \Delta \varepsilon_{re1}^I(t) &= \varepsilon_{cr}^I(t_a) - \varepsilon_{re}^I(t) \\ &= g_0^I D_0 \sigma^I \\ &+ \left\{ \begin{aligned} &g_1^I g_2^I \sigma^I \sum_{n=1}^{N_{pr}} D_n \left[1 - \exp(-\lambda_n \frac{t_a}{a_\sigma^I}) \right] \\ &- g_2^I \sigma^I \sum_{n=1}^{N_{pr}} D_n \left[1 - \exp(-\lambda_n \frac{t}{a_\sigma^I}) \right] \\ &+ g_2^I \sigma^I \sum_{n=1}^{N_{pr}} D_n \left[1 - \exp(-\lambda_n \frac{t-t_a}{a_\sigma^I}) \right] \end{aligned} \right\} \end{aligned} \quad (13)$$

246 The unknown linear viscoelastic coefficients D_0 , D_n and λ_n ($n = 1, 2, \dots, N_{pr}$) were obtained
247 from the first creep-recovery cycle by minimizing the error between the experimental mea-
248 surements and Eq. 13 using nonlinear least squares fit for each sample. The number of Prony

249 terms, $N_{pr} = 3$, was found to be sufficient to accurately represent the experimental viscoelas-
 250 tic strain response for all the samples. Also, the viscoelastic recovery compliance in the first
 251 cycle was obtained by dividing the $\Delta \varepsilon_{re1}^I$ with σ^I .

252 The total strain components for the second loading cycle, during creep and recovery
 253 phases, were obtained as

$$\begin{aligned}
 \varepsilon_{cr}^{II}(t) = & g_0^{II} D_0 \sigma^{II} \\
 & + g_1^{II} \left\{ g_2^I \sigma^I \Delta D \left(\frac{t}{a_\sigma^I} \right) - g_2^I \sigma^I \Delta D \left(\frac{t-t_a}{a_\sigma^I} \right) \right. \\
 & \left. + g_2^{II} \sigma^{II} \Delta D \left(\frac{t-t_b}{a_\sigma^{II}} \right) \right\} \\
 & + \varepsilon_{irrec}^{II}(t)
 \end{aligned} \tag{14}$$

255

$$\begin{aligned}
 \varepsilon_{re}^{II}(t) = & \left\{ g_2^I \sigma^I \Delta D \left(\frac{t}{a_\sigma^I} \right) - g_2^I \sigma^I \Delta D \left(\frac{t-t_a}{a_\sigma^I} \right) \right. \\
 & \left. + g_2^{II} \sigma^{II} \Delta D \left(\frac{t-t_b}{a_\sigma^{II}} \right) - g_2^{II} \sigma^{II} \Delta D \left(\frac{t-t_c}{a_\sigma^{II}} \right) \right\} \\
 & + \varepsilon_{irrec}^{II}(t_c)
 \end{aligned} \tag{15}$$

257 Using the previously known Prony coefficients, the unknown nonlinear VE parameters for
 258 second cycle need to be evaluated. In order to achieve this, the irrecoverable strain $\varepsilon_{irrec}^{II}(t)$
 259 at $t = t_c$ in the second cycle needs to be eliminated by manipulating Eq. 14 and 15. By sub-
 260 tracting the total strain during recovery period $\varepsilon_{re}^{II}(t)$ from itself at time $t = t_2$, the resulting

261 equation $\Delta \varepsilon_{re2}^{II}(t)$, $t_2 < t < t_d$ contains only two unknown parameters g_2^{II} and a_{σ}^{II} as follows

$$\begin{aligned}
 \Delta \varepsilon_{re2}^{II}(t) &= \varepsilon_{re}^{II}(t_2) - \varepsilon_{re}^{II}(t) \\
 &= g_2^I \sigma^I \left\{ \begin{array}{l} \sum_{n=1}^{N_{pr}} D_n \left[1 - \exp\left(-\lambda_n \frac{t_2}{a_{\sigma}^I}\right) \right] \\ - \sum_{n=1}^{N_{pr}} D_n \left[1 - \exp\left(-\lambda_n \frac{t_2 - t_d}{a_{\sigma}^I}\right) \right] \\ - \sum_{n=1}^{N_{pr}} D_n \left[1 - \exp\left(-\lambda_n \frac{t}{a_{\sigma}^I}\right) \right] \\ + \sum_{n=1}^{N_{pr}} D_n \left[1 - \exp\left(-\lambda_n \frac{t - t_d}{a_{\sigma}^I}\right) \right] \end{array} \right\} \\
 &+ g_2^{II} \sigma^{II} \left\{ \begin{array}{l} \sum_{n=1}^{N_{pr}} D_n \left[1 - \exp\left(-\lambda_n \frac{t_2 - t_b}{a_{\sigma}^{II}}\right) \right] \\ - \sum_{n=1}^{N_{pr}} D_n \left[1 - \exp\left(-\lambda_n \frac{t_2 - t_c}{a_{\sigma}^{II}}\right) \right] \\ - \sum_{n=1}^{N_{pr}} D_n \left[1 - \exp\left(-\lambda_n \frac{t - t_b}{a_{\sigma}^{II}}\right) \right] \\ + \sum_{n=1}^{N_{pr}} D_n \left[1 - \exp\left(-\lambda_n \frac{t - t_c}{a_{\sigma}^{II}}\right) \right] \end{array} \right\}
 \end{aligned} \tag{16}$$

263 These parameters g_2^{II} and a_{σ}^{II} were obtained by minimizing the error between measurements
 264 of $\Delta \varepsilon_{re2}^{II}$ as shown in Fig. 1 and Eq. 16 using nonlinear least squares method. By taking the
 265 difference between the creep strain $\varepsilon_{cr}^{II}(t_c)$ at $t = t_c$ and the strain during recovery period
 266 $\varepsilon_{re}^{II}(t)$ at time t in the second cycle, the term $\Delta \varepsilon_{re1}^{II}$ can be obtained as

$$\begin{aligned}
 \Delta \varepsilon_{re1}^{II}(t) &= \varepsilon_{cr}^{II}(t_c) - \varepsilon_{re}^{II}(t) \\
 &= g_0^{II} D_0 \sigma^{II} \\
 &+ g_1^{II} \left\{ \begin{array}{l} g_2^I \sigma^I \sum_{n=1}^{N_{pr}} D_n \left[1 - \exp\left(-\lambda_n \frac{t_c}{a_{\sigma}^I}\right) \right] \\ - g_2^I \sigma^I \sum_{n=1}^{N_{pr}} D_n \left[1 - \exp\left(-\lambda_n \frac{t_c - t_d}{a_{\sigma}^I}\right) \right] \\ + g_2^{II} \sigma^{II} \sum_{n=1}^{N_{pr}} D_n \left[1 - \exp\left(-\lambda_n \frac{t_c - t_b}{a_{\sigma}^{II}}\right) \right] \end{array} \right\} \\
 &- \left\{ \begin{array}{l} g_2^I \sigma^I \sum_{n=1}^{N_{pr}} D_n \left[1 - \exp\left(-\lambda_n \frac{t}{a_{\sigma}^I}\right) \right] \\ - g_2^I \sigma^I \sum_{n=1}^{N_{pr}} D_n \left[1 - \exp\left(-\lambda_n \frac{t - t_d}{a_{\sigma}^I}\right) \right] \\ + g_2^{II} \sigma^{II} \sum_{n=1}^{N_{pr}} D_n \left[1 - \exp\left(-\lambda_n \frac{t - t_b}{a_{\sigma}^{II}}\right) \right] \\ - g_2^{II} \sigma^{II} \sum_{n=1}^{N_{pr}} D_n \left[1 - \exp\left(-\lambda_n \frac{t - t_c}{a_{\sigma}^{II}}\right) \right] \end{array} \right\}
 \end{aligned} \tag{17}$$

268 The remaining two parameters g_0^{II} and g_1^{II} were obtained by minimizing the error between
 269 the measurements of $\Delta \varepsilon_{re1}^{II}(t)$ and Eq. 17. By applying the similar procedure to subsequent

loading cycles the associated nonlinear VE parameters were evaluated in all loading cycles. Once all the nonlinear viscoelastic parameters were obtained, the irrecoverable strain response during the loading phase was obtained from Eq. 11 for N th cycle as

$$\varepsilon_{irrec}^N(t) = \varepsilon_{cr}^N(t) - \varepsilon_{nve}^N(t) \quad (18)$$

where $N = I, II, III, \dots$ = loading cycle number. This procedure leads to nonlinear VE parameters that are known at discrete stress levels (σ^N), and these parameters can be expressed as functions of stress through interpolation or regression.

2.5 Curve fitting-nonlinear VE parameters

Once all the nonlinear VE parameters were obtained at multiple stress levels, they were fitted with appropriate functions of stress. In this study we expressed the nonlinear VE parameters as smooth second order polynomial functions of effective or von Mises stress (σ_{eff}).

$$g_0 = 1 + \sum_i^2 \alpha_i \left\langle \frac{\sigma_{eff}}{\sigma_0} - 1 \right\rangle^i \quad (19)$$

$$g_1 = 1 + \sum_i^2 \beta_i \left\langle \frac{\sigma_{eff}}{\sigma_0} - 1 \right\rangle^i \quad (20)$$

$$g_2 = 1 + \sum_i^2 \gamma_i \left\langle \frac{\sigma_{eff}}{\sigma_0} - 1 \right\rangle^i \quad (21)$$

$$a_\sigma = 1 + \sum_i^2 \delta_i \left\langle \frac{\sigma_{eff}}{\sigma_0} - 1 \right\rangle^i \quad (22)$$

where

$$\langle x \rangle = \begin{cases} x & x > 0 \\ 0 & x \leq 0 \end{cases}$$

In our uniaxial MLCR tests, σ_{eff} is equal to the applied uniaxial stress in each loading cycle. The coefficients α_i , β_i , γ_i and δ_i ($i = 1, 2$) were evaluated by fitting the Eqs. 19 - 22 to the obtained values of the parameters g_0 , g_1 , g_2 and a_σ , respectively, in all loading cycles

291 of MLCR tests on each trabecular bone sample. σ_0 (or σ^l) is the stress in the first loading
292 cycle where linear viscoelastic parameters were determined for each sample. The above
293 methodology for identification of nonlinear viscoelastic parameters is shown concisely as a
294 flowchart in Fig. 2.

295 **3 Results**

296 **3.1 MLCR experimental data**

297 A total of 19 samples were subjected to MLCR tests and the range of BV/TV of the bone
298 samples was 0.15 to 0.54. As discussed earlier our methods involved application of stress
299 corresponding to eight different strain levels. Out of the 19 samples tested 4 failed (started
300 displaying tertiary creep) in loading cycle VI, 4 in loading cycle VII and 9 in loading cycle
301 VIII. Only 2 samples survived all eight stress levels. Typical creep-recovery responses along
302 with the applied load cycles for two samples are shown in Fig. 3. These samples had a
303 BV/TV of 0.25 and 0.46 and were consequently named as S25 and S46. Five cycles of
304 loading (each followed by unloading) with the stress magnitudes of 0.64, 1.19, 1.77, 2.23,
305 2.43 MPa were applied to S25 and, similarly, six cycles with stress magnitudes of 1.75,
306 4.38, 7.45, 10.76, 14.06, 22.92 MPa were applied to S46 as shown in Figs. 3(a) and 3(b)
307 respectively. The last cycle in each sample where tertiary creep or failure was observed was
308 omitted in the analysis and also not shown in the figures. Results for all samples are provided
309 in Table 1.

310 3.2 Viscoelastic recovery compliance

311 The viscoelastic recovery compliance was evaluated in all cycles using $\Delta\varepsilon_{re1}^N/\sigma^N$ (note that
312 the numerator does not include irrecoverable strains) for all samples. Typical variation of
313 compliance with time as well as with varying applied stress is shown in Figs. 4(a)-4(d)
314 for samples S25, S33 and S46. The units for compliance are 1/MPa. In the first loading
315 cycle, for the three typical samples, the viscoelastic recovery compliance increased by 11%
316 (from 3.17×10^{-3} to 3.51×10^{-3}), 6% (from 1.40×10^{-3} to 1.48×10^{-3}) and 12% (from
317 1.00×10^{-3} to 1.12×10^{-3}) at 600 s (end of unloading phase) for samples S25, S33 and S46
318 respectively (Fig. 4). Compliance was found to increase with time in all loading cycles as
319 expected in viscoelastic material. However, the compliance for trabecular bone also found to
320 vary with stress indicating a nonlinear viscoelastic response. For sample S25, the compliance
321 increased from 3.51×10^{-3} at the end of cycle I to 4.40×10^{-3} at the end of cycle V. For
322 high density sample S46 the compliance decreased from 1.12×10^{-3} at the end of cycle I to
323 0.71×10^{-3} at the end of cycle VI. But in the sample S33, the compliance was found to first
324 decrease from 1.48×10^{-3} at the end of cycle I to 1.25×10^{-3} at the end of loading cycle IV
325 and then increase to 1.70×10^{-3} at the end of cycle VII. This stress dependent compliance
326 behaviour is shown in Fig. 4(d) for the three samples. Figure 4(e) shows that compliance
327 increases with stress for low BV/TV samples, decreases with stress for high BV/TV samples
328 and first decreases with stress and then increases with stress for mid-BV/TV samples.

329 3.3 Nonlinear viscoelastic parameters

330 The stress-dependent nonlinear viscoelastic parameters, g_0 , g_1 , g_2 and a_σ , were evaluated
331 for all 19 samples. Fig. 5(a) and 5(b) show the variation of these parameters for samples
332 S25 and S46, respectively. The procedure assumes linear viscoelasticity in the first cycle

333 (initial apparent strain of 0.2%). Numerical values of stress-dependent nonlinear viscoelas-
334 tic parameters along with other evaluated values are presented in Table 1 for all 19 samples.
335 The results show that for sample S25 the values of g_0 , g_2 and a_σ first decrease and then in-
336 crease with the stress level, whereas the value of g_1 first increases slightly and then decreases
337 slightly with the stress level (Fig. 5(a)). The product of g_1g_2 which affects the transient re-
338 sponse was also found to first decrease and then increase. These observations led us to the
339 choice of a second order polynomial function to represent the nonlinear VE parameters as
340 functions of effective stress. These second order functions produced coefficients of determi-
341 nation of $r^2 = 0.97, 0.72, 0.98$ and 0.69 for parameters g_0 , g_1 , g_2 and a_σ , respectively, as
342 shown in Fig. 5(a).

343 For sample S46, Fig. 5(b), the parameters g_0 , g_1 , g_2 were found to decrease and then
344 increase with the stress level, and a_σ was almost constant (≈ 1) and then decreased in the last
345 stress cycle. The second order polynomial functions of effective stress produced r^2 values of
346 $0.83, 0.90, 0.92$, and 0.93 for g_0 , g_1 , g_2 and a_σ , respectively for sample S46. The increase
347 in the values of g_0 , g_1 , g_2 or the product of g_1g_2 essentially means that the trabecular bone
348 material experiences viscoelastic softening (reduction of stiffness) and decrease of these
349 parameters imply that the material experiences stiffening.

350 Figures. 6(a), 6(b), 6(c) and 6(d) show the variation of nonlinear VE parameters, g_0 , g_1 ,
351 g_2 and a_σ , respectively, which were expressed as polynomial functions of effective stress,
352 for all samples. It can be seen that the variation described for two typical samples is largely
353 followed by all.

3.4 Irrecoverable strains

The irrecoverable strain along with nonlinear viscoelastic (recoverable) strain response for samples S25 and S46 are shown in Figs. 7(a) and 7(b). The figures also show the measured experimental strain response which comprises of the recoverable and irrecoverable strain components (Eq. 1). The viscoelastic strain was found to recover fully (below $7 \mu\epsilon$) in under 10 minutes during the recovery phase of each loading cycle. Irrecoverable strains exist even at the end of the first loading cycle (stress level corresponding to strain of 0.2%) and were found to increase with stress. For sample S25, the irrecoverable strain increased to 0.20% by the end of cycle V from 0.03% in cycle I, Fig. 7(a), whereas for sample S46, it increased to 0.12% by the end of loading cycle VI from 0.03% in cycle I, Fig. 7(b). The irrecoverable strains in each loading cycle for all 19 samples are shown in Fig. 8(a).

There were no significant correlations found between the irrecoverable strains and BV/TV in the loading cycles I-IV. However, a weak but significant power law correlation ($y = 0.0757x^{-0.61}$, $r^2 = 0.34$, $p < 0.001$) in the cycle V with BV/TV was found. At loading cycles at higher stress, strong and significant power law relationships $y = 0.0177x^{-2.93}$ ($r^2 = 0.78$, $p < 0.001$) and $y = 0.0862x^{-1.78}$ ($r^2 = 0.73$, $p < 0.001$) were found between the irrecoverable strains and BV/TV in the cycles VI and VII, respectively.

4 Discussion

This study developed a novel methodology to evaluate time-dependent properties of trabecular bone. Our creep-recovery experiments at multiple stress levels demonstrate that the response of trabecular bone to mechanical forces is time-dependent and the strain always comprises of recoverable and irrecoverable components even at low stress levels. Our re-

376 sults show that the viscoelastic behaviour of trabecular bone varies nonlinearly with the
377 applied stress.

378 Stress-dependence of creep response has been previously examined in studies on poly-
379 mers and concretes (Lai and Bakker, 1995; Huang et al, 2011). In these studies the creep-
380 recovery tests were conducted independently and involved long relaxation periods between
381 stress cycles. We performed creep and recovery tests at varying load levels continuously
382 without resting the sample in between the tests. We chose this protocol, as it was not ap-
383 parent how long different trabecular bone samples would take to to fully recover from any
384 loading cycle. The adopted methodology required the residual strains from the previous
385 cycle to be taken into account when evaluating the response of the following loading cycle.

386 The identification of viscoelastic parameters constitutes a two-step process. In the first
387 step, the Prony coefficients associated with linear viscoelastic response are determined for
388 the loading cycle at the lowest stress level, and in second step the linear viscoelastic re-
389 sponse with additional appropriate constitutive parameters is manipulated to match-up with
390 the experimental response at multiple stress levels using nonlinear least square minimisation
391 technique; thereby the corresponding constitutive parameters are evaluated at multiple load
392 levels. A major strength of our methodology is that it permits separation of the recoverable
393 response from the total strain response through the use of creep and recovery parts of the
394 curves in each loading cycle. Thus, it is possible to assess accurately the viscoelastic re-
395 sponse of trabecular bone. Linear viscoelastic properties were characterized by the Prony
396 series based on the generalized 3-term Kelvin model at the lowest stress cycle (correspond-
397 ing to 0.2% of applied static strain), assuming bone behaves linearly at this small strain. The
398 nonlinear viscoelastic parameters were successfully fitted to polynomial functions which
399 represent the parameters as continuous functions of stress levels. Previous studies have also

400 reported that the time-dependent behaviour of the trabecular bone is nonlinear (Deligianni
401 et al, 1994; Bowman et al, 1994; Yamamoto et al, 2006; Quaglini et al, 2009).

402 The viscoelastic recovery compliance was found to vary with time as well as with the
403 applied stress demonstrating the nonlinear stress-dependent viscoelastic response of trabec-
404 ular bone (Fig. 4). The samples with medium BV/TV (e.g S33, Fig. 4(b)) show an initially
405 decreasing and then increasing viscoelastic recovery compliance with increasing stress.
406 This indicates that the sample first becomes stiffer and then experiences softening (stiff-
407 ness degradation). This could be due to the reorganisation of the micro or ultrastructural
408 components in the bone matrix to make it stiffer initially followed by localised buckling
409 and/or damage of trabeculae causing softening. Nair et al (2014) conducted compressive
410 tests on mineralized and non-mineralized collagen microfibrils at molecular level at differ-
411 ent compressive stress levels and found that the elastic modulus of mineralized collagen
412 fibril increases significantly (stiffening) as the applied compressive load increases whereas
413 the nonmineralized samples showed reduced elastic modulus (higher deformability) with in-
414 crease in load. Our study demonstrates that this stiffening at ultrastructural level translates to
415 macro-level stiffening behaviour. Similarly, excessive deformation at molecular level may
416 break the bonds between organic and inorganic phases which can result in micro-damage
417 which manifests itself as softening at the apparent level. In general, for low BV/TV sam-
418 ples softening initiates at low stress levels (e.g. S25, Fig. 4(a)), whereas the high BV/TV
419 samples indicate stiffening with little or no degradation even at the higher stress levels at
420 which they were tested (Fig. 4(c)). Thus, micro/ultrastructural reorganisation and localised
421 buckling and/or damage may make a varying contribution (with BV/TV playing an impor-
422 tant role) to the apparent stiffening-softening behaviour with increasing stress. At higher
423 strain levels, the collective effect of buckling and damage in the individual trabeculae will
424 become dominant resulting in failure or tertiary creep. Previous studies have reported that

425 the presence of marrow may also result in hydraulic stiffening (Cowin, 1999) at higher
426 strain-rates. However, the unconfined MLCR experiments in our study were conducted at
427 relatively low strain rates (0.01 s^{-1}), and it is unlikely that marrow would have played a
428 role in the observed stiffening phenomena. Kim et al (2012) reported that the post-creep
429 unloading modulus is significantly higher than pre-creep loading modulus indicating that
430 the stiffening of trabecular bone occurs under compressive creep, and authors attributed this
431 behaviour to the possible reorganization of micro or ultrastructural components in the bone.
432 Our study also found similar stiffening at first and then softening under compressive creep.

433 All samples showed similar convex shape (Fig. 6(a)) for parameter g_0 , which affects
434 the instantaneous response, depending on their BV/TV with the coefficients of determina-
435 tion (r^2) of the polynomial functions were in the range of 0.18 to 0.99. The product of the
436 parameters g_1 and g_2 which affects the transient response, Fig. 6(e), produced the r^2 value
437 in the range of 0.37-0.99. Some of the second order polynomial functions of g_0 and g_1g_2
438 for some samples were weakly correlated, however, all of the correlations were positive
439 and showed an initially decreasing and then increasing trend, which implies decreasing and
440 increasing trend in the instantaneous and transient responses (recoverable compliance), re-
441 spectively, with increasing stress. These functions of stress-dependent parameters explain
442 the stiffening-softening behaviour of trabecular bone well under compressive creep loading.
443 The change in parameter a_σ shows the nonlinearity in the time-shift factor as a function of
444 stress. The approximations using second order polynomial functions of stress were consid-
445 ered appropriate as we had only data points corresponding to 5 to 8 stress levels.

446 The outstanding fact about these approximations is that all the functions revealed a
447 stiffening-softening behaviour for all trabecular bone samples with varying degrees of suc-
448 cess. With increasing stress the parameter g_0 and the product g_1g_2 reduce to less than 1
449 indicating stiffening (or reduced compliance) followed by an increase beyond 1 indicat-

ing softening (or increased compliance) with the further increase in stress. This can be clearly seen Fig. 6 and it can be observed that the viscoelastic response of samples with lower BV/TV was significantly different from samples with higher BV/TV. In general for lower the BV/TV samples the parameters reach their minima and increase to greater than 1 rapidly, indicating quicker stiffening-softening behaviour with stress. For samples with higher BV/TV the same behaviour was observed to vary more slowly with stress. From our results, it appears BV/TV is a good predictor of nonlinear stress-dependent viscoelastic response of the trabecular bone.

Irrecoverable strains (Fig. 8(a)) were found to exist even at smaller load levels. These strains existed consistently in all the samples and were of similar magnitudes in their first loading cycles. We believe these strains occur due to the material being loaded to strains beyond its yield point in some localised regions and entering the realm of irreversible deformation. Kim et al (2012) reported that the residual strain, which they defined as strain that remain at the end of the unloading phase, of $1797 \pm 1391 \mu\epsilon$ remained after 2 hours of strain recovery in the unloading phase when the plateau force corresponding to static strain of $2000 \mu\epsilon$ was applied in a creep test. Yamamoto et al (2006) also reported residual strains and found that their magnitude was of a similar magnitude to the applied static strain ($515 \pm 255 \mu\epsilon$ and 1565 ± 590 for applied static strains of 750 and 1500 $\mu\epsilon$, respectively) at the end 35 hours of recovery period. From this they estimated that these residual strains will fully recover in 26 to 63 days. Our study concludes that these residual strains are, in fact, irrecoverable (permanent) strains and never recover *in vitro*. We applied plateau load only for 200 s, the resulting irrecoverable strain magnitudes at the end of unloading phase (600 s of strain recovery) were of the order of 242 $\mu\epsilon$ to 1267 $\mu\epsilon$ in the first loading cycle where applied plateau load corresponds to static strain of 2000 $\mu\epsilon$, consistent with those observed in the previous studies (Yamamoto et al, 2006; Kim et al, 2012). However, *in vivo*, since

475 bone is a living tissue, microdamage (which is the cause of these permanent strains) is likely
476 to be repaired and replaced by a newer bone material via remodelling. In fact, microdamage
477 in bone acts as a stimulus for directing biological activity (Burr et al, 1985; Lee et al, 2002).
478 The microdamage initiates at scales below the macroscopic porosity of the bone, and may
479 be affected by intrinsic viscoelasticity of the tissue phase. The newly formed material due
480 to bone remodelling may have less mineral which may increase compliance locally. The
481 overall viscoelastic response at apparent level represents an average of old and new bone.

482 Kim et al (2012) also reported from their experimental creep tests that the loading creep
483 rate (during plateau load) is significantly higher than the unloading creep rate (during strain
484 recovery in unloading phase) in trabecular bone. This possibly indicates that the creep re-
485 sponse during plateau loading contains evolution of not only recoverable strain but also
486 some irreversible strain response. Our study validates this phenomenon and concludes that
487 the creep response of the trabecular bone always contains both recoverable and irrecoverable
488 responses even at smaller strains/stresses.

489 These irrecoverable strains at lower loading cycles (I-IV) were found to have no correla-
490 tion with BV/TV. However, as the applied plateau loads increase in the higher loading cycles
491 (V-VII) these strains strongly depend on BV/TV, Fig. 8(b). Samples with lower BV/TV ex-
492 perience higher irreversible strains with power law relationships, and irreversible strains
493 decreased with the increasing BV/TV at the same applied strain level, Fig. 8(b).

494 The mechanisms driving the viscoelastic behaviour in trabecular bone are not yet com-
495 pletely understood. It has been speculated that the individual constituents at different hier-
496 archical levels in the trabecular bone and its microstructure contribute to the viscoelastic
497 behaviour at the specimen level. Linde (1994) pointed out that the viscoelastic response of
498 trabecular bone may depend on both the presence of marrow within the tissue and properties
499 of the tissue itself, and Bowman et al (1999) suggested that the collagen phase is responsible

500 for the creep behaviour of the trabecular bone. Nair et al (2014) suggested that extrafibrillar
501 mineralization is mandatory along with intrafibrillar mineralization to provide the required
502 bone mechanical properties. Further investigations are required to explicitly quantify the
503 contributions of individual constituents to the apparent level viscoelastic behaviour of bone.
504 However, from our results, it is evident that the BV/TV plays a major role in predicting the
505 apparent level viscoelastic behaviour (Manda et al, 2016).

506 This work can be incorporated in finite element (FE) programs by coding a user defined
507 material (UMAT) subroutine based on Schapery's single integral model (Schapery, 1969),
508 which is not generally available in commercial FE packages. The linear Prony coefficients
509 and the stress dependent nonlinear VE parameters reported in Table 1 will act as input to
510 the UMAT. The nonlinear VE parameters need to be supplied as smooth functions of stress
511 (Eqs. 19 - 22).

512 Our study also has a few limitations. Firstly, it is not possible in practice to perform ideal
513 creep-recovery experiments, and in our tests the time intervals during the ramp loading and
514 unloading are finite (1 s to reach 1.0% strain with the strain rate of 0.01 s^{-1}). Small vis-
515 coelastic deformations are likely to occur during the ramp loading phase; it may be possible
516 to include these in a more elaborate model. In this study finite ramp loading/unloading was
517 treated as instantaneous in our material model; we believe this assumption has negligible
518 effect on the evaluated material parameters. Our creep tests were performed with the plateau
519 load holding time of 200 s which we believe is sufficiently long in comparison to the ramp
520 loading/unloading time it will have a negligible effect on the measured creep response. As
521 in many previous studies our experiments were performed at room temperature. It is possi-
522 ble that increase in temperature to $37 \text{ }^\circ\text{C}$ may have a small effect on the creep behaviour;
523 currently the published data to confirm or invalidate this is limited.

524 **5 Compliance with Ethical Standards**

525 The proximal bovine femora used in this study were obtained from a local abattoir.

526 **6 Funding**

527 This study was funded by the Engineering and Physical Sciences Research Council (grant
528 number EP/K036939/1).

529 **7 Conflict of Interest**

530 None of the authors have any conflicts of interest to report with respect to the material
531 contained in this manuscript.

532 **Acknowledgements** The authors are grateful to the Engineering and Physical Sciences Research Council
533 (EPSRC) grant EP/K036939/1.

534 **References**

- 535 Bowman SM, Keaveny TM, Gibson LJ, Hayes WC, McMahon TA (1994) Compressive
536 creep behavior of bovine trabecular bone. *Journal of Biomechanics* 27(3):301–305, 307–
537 310
- 538 Bowman SM, Guo XE, Cheng DW, Keaveny TM, Gibson LJ, Hayes WC, McMahon TA
539 (1998) Creep contributes to the fatigue behavior of bovine trabecular bone. *Journal of*
540 *Biomechanical Engineering* 120(5):647–654
- 541 Bowman SM, Gibson LJ, Hayes WC, McMahon TA (1999) Results from demineralized
542 bone creep tests suggest that collagen is responsible for the creep behavior of bone. *Jour-*
543 *nal of Biomechanical Engineering* 121(2):253–258

-
- 544 Bredbenner TL, Davy DT (2006) The effect of damage on the viscoelastic behavior of hu-
545 man vertebral trabecular bone. *Journal of Biomechanical Engineering* 128(4):473–480
- 546 Burr DB, Martin RB, Schaffler MB, Radin EL (1985) Bone remodeling in response to in
547 vivo fatigue microdamage. *Journal of Biomechanics* 18(3):189–200
- 548 Christensen RM (1980) Nonlinear theory of viscoelasticity for application to elastomers.
549 *Journal of Applied Mechanics, Transactions ASME* 47(4):762–768
- 550 Cowin SC (1999) Bone poroelasticity. *Journal of Biomechanics* 32(3):217–238
- 551 Currey JD (1986) Power law models for the mechanical properties of cancellous bone. *En-
552 gineering in medicine* 15(3):153–154
- 553 Deligianni DD, Maris A, Missirlis YF (1994) Stress relaxation behaviour of trabecular bone
554 specimens. *Journal of Biomechanics* 27(12):1469–1476
- 555 Dillard DA, Straight MR, Brinson HF (1987) The nonlinear viscoelastic characterization of
556 graphite/epoxy composites. *Polymer Engineering & Science* 27(2):116–123
- 557 Findley W, Lai J, Onaran K (1976) Creep and relaxation of nonlinear viscoelastic materials,
558 with an introduction to linear viscoelasticity. North-Holland series in applied mathematics
559 and mechanics, North-Holland Pub. Co.
- 560 Goffin JM, Pankaj P, Simpson AH (2013) The importance of lag screw position for the
561 stabilization of trochanteric fractures with a sliding hip screw: A subject-specific finite
562 element study. *Journal of Orthopaedic Research* 31(4):596–600
- 563 Guedes RM, Simes JA, Morais JL (2006) Viscoelastic behaviour and failure of bovine can-
564 cellous bone under constant strain rate. *Journal of Biomechanics* 39(1):49–60
- 565 Huang C, Abu Al-Rub RK, Masad EA, Little DN, Airey GD (2011) Numerical implemen-
566 tation and validation of a nonlinear viscoelastic and viscoplastic model for asphalt mixes.
567 *International Journal of Pavement Engineering* 12(4):433–447

-
- 568 Keaveny TM, Pinilla TP, Crawford RP, Kopperdahl DL, Lou A (1997) Systematic and ran-
569 dom errors in compression testing of trabecular bone. *Journal of Orthopaedic Research*
570 15(1):101–110
- 571 Keaveny TM, Morgan EF, Niebur GL, Yeh OC (2001) Biomechanics of trabecular bone.
572 *Annual Review of Biomedical Engineering* 3:307–333
- 573 Kim DG, Navalgund AR, Tee BC, Noble GJ, Hart RT, Lee HR (2012) Increased variability
574 of bone tissue mineral density resulting from estrogen deficiency influences creep behav-
575 ior in a rat vertebral body. *Bone* 51(5):868 – 875
- 576 Kim DG, Huja SS, Navalgund A, DAtri A, Tee B, Reeder S, Lee HR (2013) Effect of
577 estrogen deficiency on regional variation of a viscoelastic tissue property of bone. *Journal*
578 *of Biomechanics* 46(1):110 – 115
- 579 Knauss WG, Emri IJ (1981) Non-linear viscoelasticity based on free volume consideration.
580 *Computers and Structures* 13(1-3):123–128
- 581 Kopperdahl DL, Keaveny TM (1998) Yield strain behavior of trabecular bone. *Journal of*
582 *Biomechanics* 31(7):601–608
- 583 Lai J, Bakker A (1995) An integral constitutive equation for nonlinear plasto-viscoelastic
584 behavior of high-density polyethylene. *Polymer Engineering & Science* 35(17):1339–
585 1347
- 586 Lee TC, Staines A, Taylor D (2002) Bone adaptation to load: Microdamage as a stimulus
587 for bone remodelling. *Journal of anatomy* 201(6):437–446
- 588 Levrero-Florencio F, Margetts L, Sales E, Xie S, Manda K, Pankaj P (2016) Evaluating
589 the macroscopic yield behaviour of trabecular bone using a nonlinear homogenisation
590 approach. *Journal of the Mechanical Behavior of Biomedical Materials* 61:384–396
- 591 Linde F (1994) Elastic and viscoelastic properties of trabecular bone by a compression test-
592 ing approach. *Danish medical bulletin* 41(2):119–138

-
- 593 Linde F, Hvid I, Pongsoipetch B (1989) Energy absorptive properties of human trabecular
594 bone specimens during axial compression. *Journal of Orthopaedic Research* 7(3):432–
595 439
- 596 Lou YC, Schapery RA (1971) Viscoelastic characterization of a nonlinear fiber- reinforced
597 plastic. *Journal of Composite Materials* 5:208–234
- 598 Manda K, Xie S, Wallace RJ, Levrero-Florencio F, Pankaj P (2016) Linear viscoelasticity -
599 bone volume fraction relationships of bovine trabecular bone. *Biomechanics and Model-*
600 *ing in Mechanobiology* pp 1–10, article in Press, DOI:10.1007/s10237-016-0787-0
- 601 Morgan EF, Yeh OC, Chang WC, Keaveny TM (2001) Nonlinear behavior of trabecular
602 bone at small strains. *Journal of Biomechanical Engineering* 123(1):1–9
- 603 Morgan EF, Bayraktar HH, Keaveny TM (2003) Trabecular bone modulus density relation-
604 ships depend on anatomic site. *Journal of Biomechanics* 36(7):897 – 904
- 605 Nair AK, Gautieri A, Buehler MJ (2014) Role of intrafibrillar collagen mineralization in
606 defining the compressive properties of nascent bone. *Biomacromolecules* 15(7):2494–
607 2500
- 608 Nordin L, Varna J (2005) Methodology for parameter identification in nonlinear viscoelastic
609 material model. *Mechanics of Time-Dependent Materials* 9(4):259–280
- 610 Norman TL, Ackerman ES, Smith TS, Gruen TA, Yates AJ, Blaha JD, Kish VL (2006)
611 Cortical bone viscoelasticity and fixation strength of press-fit femoral stems: An in-vitro
612 model. *Journal of Biomechanical Engineering* 128(1):13–17
- 613 Phillips A, Pankaj P, May F, Taylor K, Howie C, Usmani A (2006) Constitutive models for
614 impacted morsellised cortico-cancellous bone. *Biomaterials* 27(9):2162–2170
- 615 Pollintine P, Luo J, Offa-Jones B, Dolan P, Adams MA (2009) Bone creep can cause pro-
616 gressive vertebral deformity. *Bone* 45(3):466–472

-
- 617 Provenzano PP, Lakes RS, Corr DT, Vanderby Jr R (2002) Application of nonlinear
618 viscoelastic models to describe ligament behavior. *Biomechanics and Modeling in*
619 *Mechanobiology* 1(1):45–57
- 620 Quaglini V, Russa VL, Corneo S (2009) Nonlinear stress relaxation of trabecular bone.
621 *Mechanics Research Communications* 36(3):275–283
- 622 Rachner TD, Khosla S, Hofbauer LC (2011) Osteoporosis: Now and the future. *The Lancet*
623 377(9773):1276–1287
- 624 Schapery RA (1969) On characterization of nonlinear viscoelastic materials. *Polymer Eng*
625 *& Science* 9(4):295–310
- 626 Schapery RA (1997) Nonlinear viscoelastic and viscoplastic constitutive equations based on
627 thermodynamics. *Mechanics Time-Dependent Materials* 1(2):209–240
- 628 Schoenfeld CM, Lautenschlager EP, Meyer PR (1974) Mechanical properties of human can-
629 cellous bone in the femoral head. *Medical and Biological Engineering* 12(3):313–317
- 630 Singh M, Nagrath AR, Maini PS (1970) Changes in trabecular pattern of the upper end
631 of the femur as an index of osteoporosis. *Journal of Bone and Joint Surgery - Series A*
632 52(3):457–467
- 633 Smart J, Williams J (1972) A comparison of single-integral non-linear viscoelasticity theo-
634 ries. *Journal of the Mechanics and Physics of Solids* 20(5):313 – 324
- 635 Yamamoto E, Paul Crawford R, Chan DD, Keaveny TM (2006) Development of residual
636 strains in human vertebral trabecular bone after prolonged static and cyclic loading at low
637 load levels. *Journal of Biomechanics* 39(10):1812–1818
- 638 Zilch H, Rohlmann A, Bergmann G, Koelbel R (1980) Material properties of femoral can-
639 cellous bone in axial loading. part ii: Time-dependent properties. *Archives of Orthopaedic*
640 *and Traumatic Surgery* 97(4):257–262

Table 1: The nonlinear VE parameters along with linear Prony coefficients and irrecoverable strains at multiple stress levels for all 19 samples. BV/TV is the bone volume fraction, D_0 is the instantaneous compliance in 1/MPa, D_n ($n = 1, 2, 3$) are transient compliance coefficients in 1/MPa, and λ_n ($n = 1, 2, 3$) are reciprocal of n th retardation time in Prony series in s^{-1} , ϵ_{static} is the applied static strain in each loading cycle, σ^N is the stress corresponding to plateau stress in the N th loading cycle in MPa. Parameters g_0, g_1, g_2, a_σ are stress-dependent nonlinear VE parameters and ϵ_{irrec} is the irrecoverable strain exist at the end of each loading cycle.

BV/TV	Linear Prony coefficients at σ^I		Cycle No.	$\epsilon_{static}[\%]$	$\sigma^N[\text{MPa}]$	Nonlinear VE parameters				$\epsilon_{irrec}[\%]$
						g_0	g_1	g_2	a_σ	
0.15	D_0	$6.40e-03$	<i>I</i>	0.20	0.36	1.00	1.00	1.00	1.00	0.041
	D_1	$5.48e-04$	<i>II</i>	0.40	0.66	0.91	1.06	0.59	0.78	0.067
	D_2	$3.24e-04$	<i>III</i>	0.60	0.94	0.94	1.03	0.67	0.82	0.104
	$D_3 =$	$2.97e-04$	<i>IV</i>	0.80	1.17	0.99	1.01	0.82	0.85	0.158
	λ_1	$8.64e-03$	<i>V</i>	1.00	1.35	1.10	0.96	0.84	0.91	0.237
	λ_2	$8.64e-01$								
0.19	D_0	$3.44e-03$	<i>I</i>	0.20	0.64	1.00	1.00	1.00	1.00	0.024
	D_1	$1.85e-04$	<i>II</i>	0.40	1.24	0.89	0.85	0.94	0.88	0.045
	D_2	$1.25e-04$	<i>III</i>	0.60	1.89	0.87	0.89	1.02	0.92	0.076
	$D_3 =$	$2.47e-04$	<i>IV</i>	0.80	2.44	0.85	0.86	1.50	0.86	0.150
	λ_1	$6.51e-01$								
	λ_2	$4.12e-02$								
	λ_3	$3.57e-03$								

Continued on next page...

BV/TV	Linear Prony coefficients at σ^I			Cycle No.	$\varepsilon_{static}[\%]$	σ^N [MPa]	Nonlinear VE parameters				$\varepsilon_{irrec}[\%]$
							g_0	g_1	g_2	a_σ	
				V	1.00	2.74	0.90	0.85	1.51	0.90	0.230
0.21	D_0	$3.42e-03$	I	0.20	0.60	1.00	1.00	1.00	1.00	0.026	
	D_1	$3.39e-04$	II	0.40	1.16	0.90	1.05	0.84	0.69	0.041	
	D_2	$3.29e-04$	III	0.60	1.73	0.87	1.06	0.82	0.69	0.062	
	$D_3 =$	$1.64e-04$	IV	0.80	2.38	0.85	1.05	0.91	0.73	0.099	
	λ_1	$6.20e-03$	V	1.00	2.82	0.88	1.04	1.11	0.73	0.161	
	λ_2	$2.42e+00$									
0.25	D_0	$3.52e-03$	I	0.20	0.64	1.00	1.00	1.00	1.00	0.032	
	D_1	$1.31e-04$	II	0.40	1.20	0.90	1.02	0.82	0.79	0.049	
	D_2	$2.63e-04$	III	0.60	1.77	0.91	1.05	0.96	0.75	0.084	
	$D_3 =$	$1.30e-04$	IV	0.80	2.23	0.98	1.04	1.19	0.74	0.140	
	λ_1	$7.57e-02$	V	1.00	2.43	1.06	1.01	1.44	0.81	0.209	
	λ_2	$6.44e-03$									
0.26	D_0	$2.68e-03$	I	0.20	0.80	1.00	1.00	1.00	1.00	0.057	
	D_1	$1.75e-04$	II	0.40	1.65	0.78	0.94	0.64	0.91	0.089	
	D_2	$1.33e-04$	III	0.60	2.48	0.77	0.99	0.71	0.88	0.116	
	$D_3 =$	$1.66e-04$	IV	0.80	3.28	0.81	0.90	0.65	0.96	0.142	
	λ_1	$7.77e-03$									
	λ_2	$1.15e-01$									
	λ_3	$1.06e+00$									

Continued on next page...

BV/TV	Linear Prony coefficients at σ^I			Cycle No.	$\varepsilon_{static}[\%]$	σ^N [MPa]	Nonlinear VE parameters				$\varepsilon_{irrec}[\%]$
							g_0	g_1	g_2	a_σ	
				V	1.00	4.01	0.83	0.89	0.79	0.97	0.186
				VI	1.50	6.50	0.82	1.01	1.86	0.86	0.960
				VII	2.00	3.62	1.02	0.94	2.14	0.96	1.041
0.33	D_0	$1.75e-03$		I	0.20	1.19	1.00	1.00	1.00	1.00	0.065
	D_1	$7.46e-05$		II	0.40	2.76	0.66	0.93	0.84	0.98	0.076
	D_2	$1.11e-04$		III	0.60	4.58	0.63	0.94	0.74	0.99	0.083
	$D_3 =$	$6.68e-05$		IV	0.80	6.40	0.62	0.92	0.71	0.98	0.091
	λ_1	$9.87e-03$		V	1.00	8.18	0.62	0.95	0.67	0.99	0.100
	λ_2	$1.02e+00$		VI	1.50	13.37	0.75	0.92	1.32	0.95	0.442
	λ_3	$1.21e-01$		VII	2.00	11.13	0.78	0.92	1.53	0.96	0.526
0.35	D_0	$1.60e-03$		I	0.20	1.31	1.00	1.00	1.00	1.00	0.039
	D_1	$1.14e-04$		II	0.40	2.69	0.84	1.14	0.71	0.67	0.057
	D_2	$6.45e-05$		III	0.60	4.09	0.84	1.08	0.60	0.78	0.072
	$D_3 =$	$8.35e-05$		IV	0.80	5.59	0.82	1.00	0.57	0.87	0.075
	λ_1	$7.64e-03$		V	1.00	7.50	0.78	1.00	0.37	0.93	0.109
	λ_2	$9.41e-02$		VI	1.50	13.01	0.70	1.02	0.66	0.80	0.214
	λ_3	$7.05e-01$									
0.35	D_0	$2.16e-03$		I	0.20	0.94	1.00	1.00	1.00	1.00	0.047
	D_1	$1.41e-04$		II	0.40	2.16	0.70	1.02	0.84	0.84	0.077
	D_2	$1.43e-04$		III	0.60	3.46	0.67	1.03	0.80	0.85	0.097
	$D_3 =$	$1.11e-04$		IV	0.80	4.67	0.65	1.02	0.75	0.86	0.118
	λ_1	$6.41e-03$									
	λ_2	$1.41e+00$									
	λ_3	$1.22e-01$									

Continued on next page...

BV/TV	Linear Prony coefficients at σ^I			Cycle No.	$\varepsilon_{static}[\%]$	σ^N [MPa]	Nonlinear VE parameters				$\varepsilon_{irrec}[\%]$
							g_0	g_1	g_2	a_σ	
				V	1.00	6.04	0.63	1.02	0.72	0.87	0.135
				VI	1.50	10.67	0.62	1.04	0.82	0.80	0.406
				VII	2.00	11.83	0.62	1.03	0.94	0.79	0.522
0.36	D_0	$2.07e-03$		I	0.20	0.98	1.00	1.00	1.00	1.00	0.073
	D_1	$1.48e-04$		II	0.40	2.12	0.71	1.20	0.45	0.70	0.087
	D_2	$1.52e-04$		III	0.60	3.67	0.65	1.02	0.43	0.87	0.112
	$D_3 =$	$1.55e-04$		IV	0.80	5.28	0.62	0.95	0.41	0.93	0.128
	λ_1	$1.63e-01$		V	1.00	7.02	0.59	0.89	0.40	0.97	0.144
	λ_2	$1.07e-02$		VI	1.50	12.73	0.54	1.00	0.42	0.89	0.244
	λ_3	$1.75e+00$		VII	2.00	16.68	0.45	1.01	0.75	0.79	0.377
0.39	D_0	$1.53e-03$		I	0.20	1.33	1.00	1.00	1.00	1.00	0.058
	D_1	$1.07e-04$		II	0.40	2.92	0.76	0.83	0.76	0.97	0.066
	D_2	$1.07e-04$		III	0.60	4.79	0.67	1.02	0.78	0.83	0.076
	$D_3 =$	$8.45e-05$		IV	0.80	6.69	0.63	1.05	0.83	0.75	0.089
	λ_1	$6.37e-03$		V	1.00	8.53	0.65	1.07	0.64	0.79	0.111
	λ_2	$1.27e+00$		VI	1.50	14.81	0.66	1.02	0.56	0.86	0.288
	λ_3	$1.23e-01$		VII	2.00	17.19	0.60	1.04	1.01	0.77	0.458
0.40	D_0	$2.88e-03$		I	0.20	0.71	1.00	1.00	1.00	1.00	0.127
	D_1	$2.36e-04$		II	0.40	1.65	0.46	0.89	0.51	0.97	0.170
	D_2	$5.01e-04$		III	0.60	2.95	0.44	0.87	0.41	0.96	0.201
	$D_3 =$	$2.56e-04$		IV	0.80	4.32	0.43	0.90	0.40	0.98	0.220
	λ_1	$1.12e-02$									
	λ_2	$2.57e+00$									
	λ_3	$1.54e-01$									

Continued on next page...

BV/TV	Linear Prony coefficients at σ^I		Cycle No.	$\varepsilon_{static}[\%]$	σ^N [MPa]	Nonlinear VE parameters				$\varepsilon_{irrec}[\%]$
						g_0	g_1	g_2	a_σ	
			V	1.00	5.74	0.43	0.91	0.34	0.99	0.227
			VI	1.50	11.56	0.39	0.92	0.36	0.94	0.346
			VII	2.00	14.98	0.39	0.90	0.33	0.97	0.491
0.40	D_0	$2.69e-03$	I	0.20	0.77	1.00	1.00	1.00	1.00	0.085
	D_1	$9.10e-05$	II	0.40	2.13	0.52	0.85	0.73	0.96	0.109
	D_2	$1.02e-04$	III	0.60	3.69	0.47	0.88	0.67	0.98	0.126
	$D_3 =$	$1.26e-04$	IV	0.80	5.35	0.43	0.96	0.70	0.91	0.141
	λ_1	$1.55e-01$	V	1.00	7.11	0.43	0.88	0.60	0.98	0.160
	λ_2	$9.68e-03$	VI	1.50	13.69	0.37	0.99	0.69	0.89	0.295
	λ_3	$1.13e+00$	VII	2.00	17.41	0.38	1.01	0.95	0.87	0.550
0.42	D_0	$1.47e-03$	I	0.20	1.37	1.00	1.00	1.00	1.00	0.037
	D_1	$1.09e-04$	II	0.40	2.97	0.73	1.03	0.98	0.83	0.054
	D_2	$8.72e-05$	III	0.60	4.74	0.71	1.04	0.86	0.82	0.059
	$D_3 =$	$7.91e-05$	IV	0.80	6.57	0.69	1.04	0.82	0.84	0.079
	λ_1	$2.81e+00$	V	1.00	8.44	0.66	1.03	0.85	0.85	0.091
	λ_2	$8.63e-03$	VI	1.50	14.45	0.67	0.91	0.68	0.96	0.158
	λ_3	$1.76e-01$	VII	2.00	19.20	0.63	1.01	0.88	0.86	0.301
0.43	D_0	$1.94e-03$	I	0.20	1.08	1.00	1.00	1.00	1.00	0.066
	D_1	$1.19e-04$	II	0.40	2.39	0.67	1.09	0.60	0.74	0.096
	D_2	$1.75e-04$	III	0.60	3.88	0.63	1.03	0.59	0.80	0.118
	$D_3 =$	$9.27e-05$	IV	0.80	5.54	0.60	1.05	0.55	0.77	0.141
	λ_1	$7.85e-01$								
	λ_2	$7.38e-03$								
	λ_3	$9.59e-02$								

Continued on next page...

BV/TV	Linear Prony coefficients at σ^I		Cycle No.	$\varepsilon_{static}[\%]$	σ^N [MPa]	Nonlinear VE parameters				$\varepsilon_{irrec}[\%]$		
						g_0	g_1	g_2	a_σ			
			<i>V</i>	1.00	7.22	0.61	0.89	0.52	0.96	0.146		
			<i>VI</i>	1.50	13.04	0.57	1.01	0.42	0.84	0.268		
			<i>VII</i>	2.00	16.91	0.55	1.00	0.51	0.85	0.406		
			<i>VIII</i>	2.50	20.56	0.56	1.00	0.57	0.86	0.608		
0.43	$\begin{bmatrix} D_0 \\ D_1 \\ D_2 \\ D_3 \\ \lambda_1 \\ \lambda_2 \\ \lambda_3 \end{bmatrix} =$	$\begin{bmatrix} 9.40e-04 \\ 3.67e-05 \\ 6.46e-05 \\ 6.43e-05 \\ 1.06e-01 \\ 6.74e-03 \\ 9.59e-01 \end{bmatrix}$	<i>I</i>	0.20	2.13	1.00	1.00	1.00	1.00	0.042		
			<i>II</i>	0.40	4.75	0.74	1.09	0.70	0.73	0.057		
			<i>III</i>	0.60	7.96	0.67	1.08	0.64	0.70	0.074		
			<i>IV</i>	0.80	11.29	0.64	1.07	0.62	0.75	0.088		
			<i>V</i>	1.00	14.65	0.61	1.06	0.68	0.78	0.102		
			<i>VI</i>	1.50	24.26	0.66	1.04	0.75	0.72	0.180		
0.46	$\begin{bmatrix} D_0 \\ D_1 \\ D_2 \\ D_3 \\ \lambda_1 \\ \lambda_2 \\ \lambda_3 \end{bmatrix} =$	$\begin{bmatrix} 1.16e-03 \\ 4.19e-05 \\ 5.82e-05 \\ 8.91e-05 \\ 6.99e-02 \\ 6.48e-03 \\ 6.75e-01 \end{bmatrix}$	<i>I</i>	0.20	1.75	1.00	1.00	1.00	1.00	0.037		
			<i>II</i>	0.40	4.38	0.68	0.92	0.78	1.00	0.043		
			<i>III</i>	0.60	7.45	0.61	0.89	0.69	0.97	0.049		
			<i>IV</i>	0.80	10.77	0.57	0.88	0.62	0.97	0.056		
			<i>V</i>	1.00	14.06	0.56	0.83	0.62	0.98	0.060		
			<i>VI</i>	1.50	22.92	0.53	1.01	0.60	0.79	0.121		
0.52	$\begin{bmatrix} D_0 \\ D_1 \\ D_2 \\ D_3 \\ \lambda_1 \\ \lambda_2 \\ \lambda_3 \end{bmatrix} =$	$\begin{bmatrix} 2.29e-03 \\ 1.74e-04 \\ 2.03e-04 \\ 1.60e-04 \\ 1.50e+00 \\ 6.85e-03 \\ 1.29e-01 \end{bmatrix}$	<i>I</i>	0.20	0.89	1.00	1.00	1.00	1.00	0.095		
			<i>II</i>	0.40	2.25	0.48	1.13	0.63	0.66	0.138		
			<i>III</i>	0.60	3.87	0.43	1.09	0.60	0.69	0.175		

Continued on next page...

BV/TV	Linear Prony coefficients at σ^I		Cycle No.	$\varepsilon_{static}[\%]$	σ^N [MPa]	Nonlinear VE parameters				$\varepsilon_{irrec}[\%]$
						g_0	g_1	g_2	a_σ	
			<i>IV</i>	0.80	5.62	0.42	1.08	0.49	0.74	0.210
			<i>V</i>	1.00	7.54	0.43	0.76	0.50	0.97	0.239
			<i>VI</i>	1.50	15.62	0.36	1.05	0.41	0.76	0.364
			<i>VII</i>	2.00	20.88	0.36	1.03	0.32	0.82	0.447
			<i>VIII</i>	2.50	26.56	0.33	1.03	0.53	0.73	0.656
0.53	D_0	$9.05e-04$	<i>I</i>	0.20	2.22	1.00	1.00	1.00	1.00	0.033
	D_1	$4.26e-05$	<i>II</i>	0.40	5.03	0.79	0.81	0.95	0.92	0.048
	D_2	$3.35e-05$	<i>III</i>	0.60	8.02	0.75	0.84	0.88	0.92	0.059
	$D_3 =$	$4.21e-05$	<i>IV</i>	0.80	11.05	0.73	0.83	0.90	0.94	0.073
	λ_1	$6.32e-01$	<i>V</i>	1.00	14.10	0.71	0.87	0.91	0.96	0.085
	λ_2	$6.40e-02$	<i>VI</i>	1.50	23.66	0.67	1.00	1.07	0.78	0.174
	λ_3	$5.54e-03$	<i>VII</i>	2.00	30.13	0.75	1.01	0.90	0.86	0.310
0.54	D_0	$1.36e-03$	<i>I</i>	0.20	1.49	1.00	1.00	1.00	1.00	0.050
	D_1	$8.02e-05$	<i>II</i>	0.40	4.00	0.58	1.06	0.71	1.00	0.058
	D_2	$6.44e-05$	<i>III</i>	0.60	7.38	0.50	1.11	0.48	1.00	0.061
	$D_3 =$	$6.17e-05$	<i>IV</i>	0.80	11.01	0.45	0.90	0.60	0.98	0.065
	λ_1	$8.56e-01$	<i>V</i>	1.00	14.66	0.45	0.87	0.47	1.00	0.074
	λ_2	$8.64e-03$	<i>VI</i>	1.50	24.90	0.42	0.96	0.49	0.88	0.129
	λ_3	$9.62e-02$								

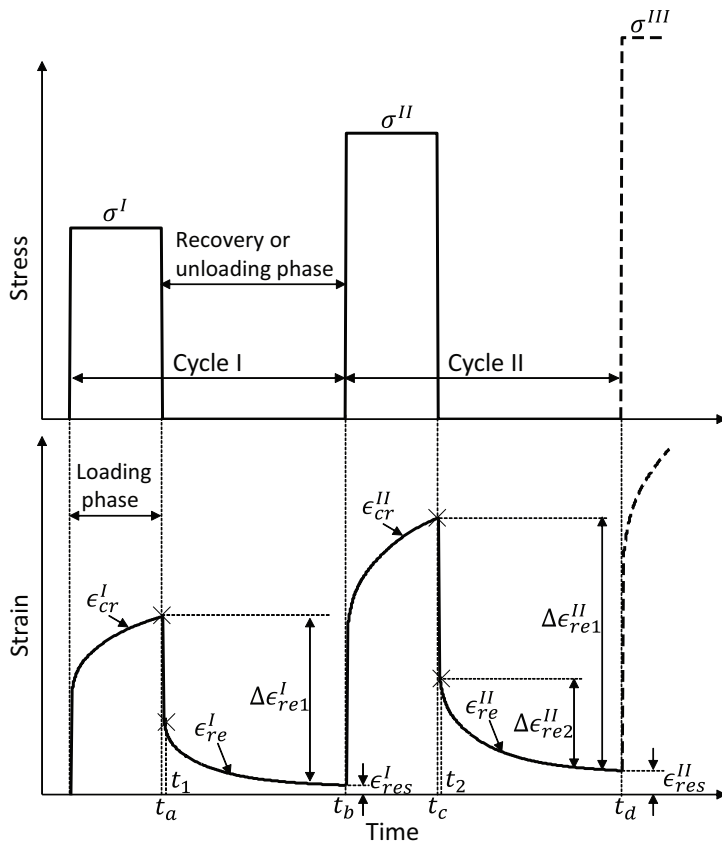


Fig. 1 A schematic representation of experimental creep and recovery tests at multiple load levels

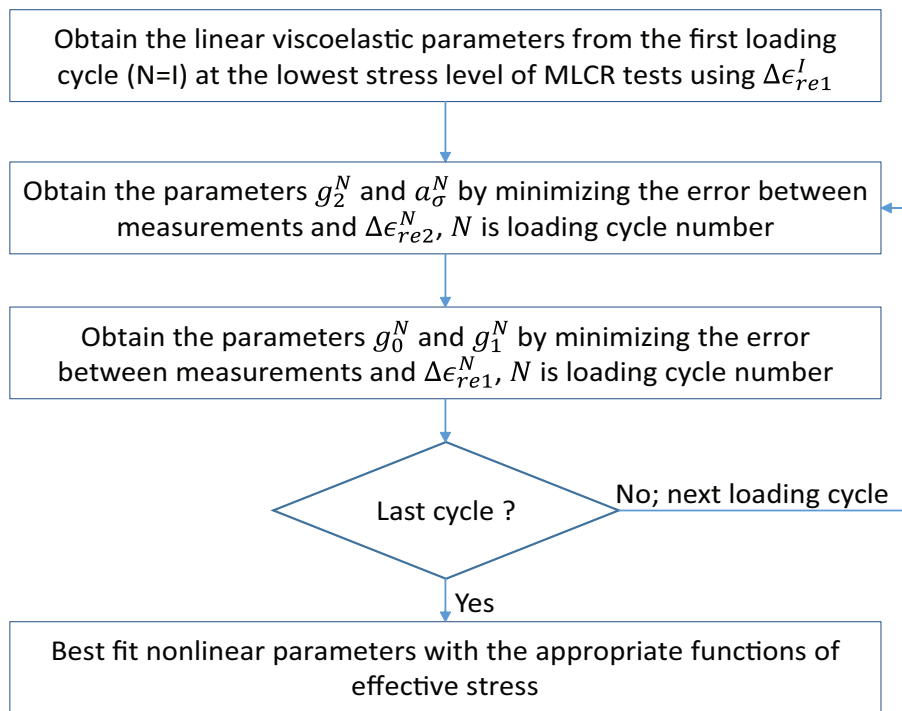
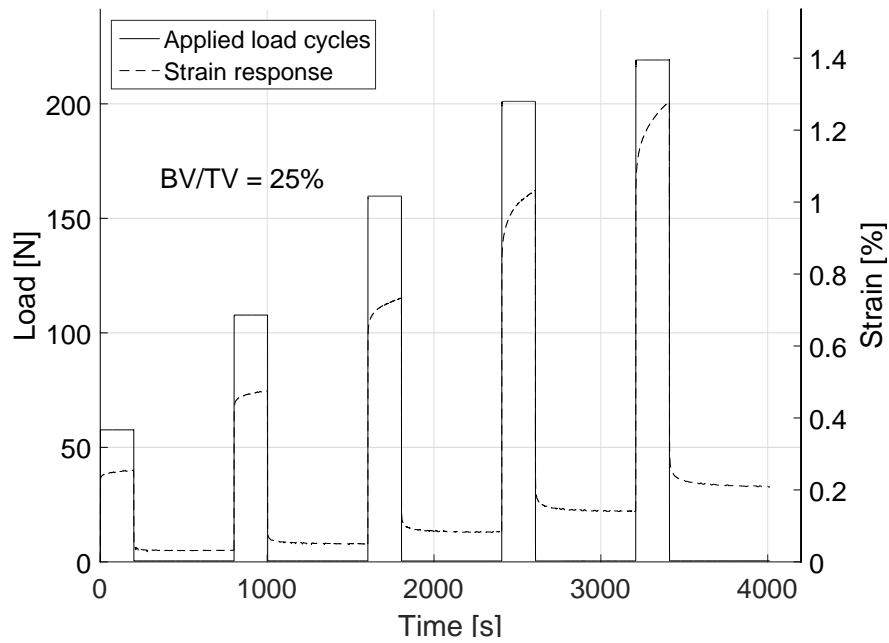
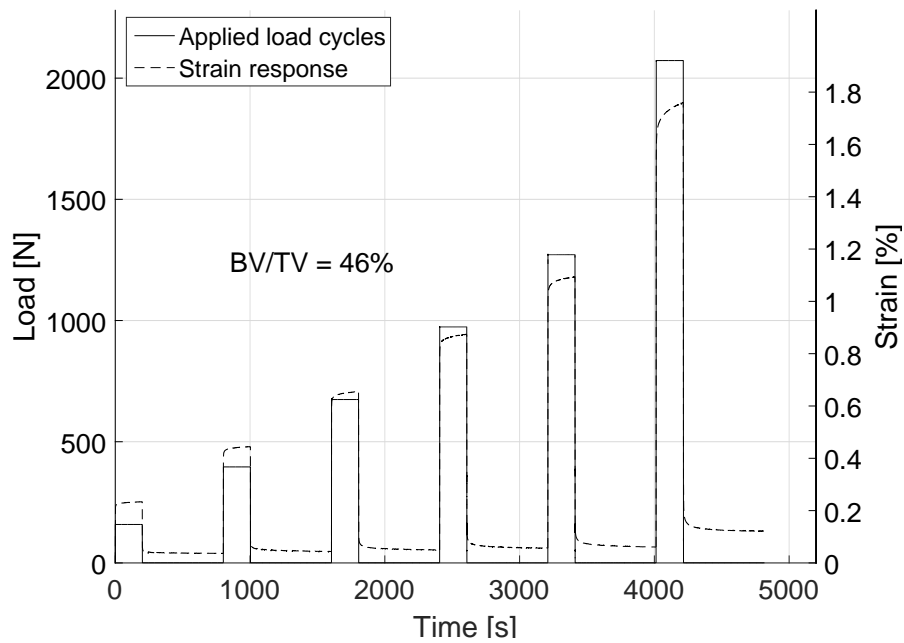


Fig. 2 Methodology for estimation of nonlinear viscoelastic parameters of trabecular bone



(a)



(b)

Fig. 3 Experimental creep-recovery responses from MLCR tests along with the applied load levels on two typical samples of (a) $BV/TV = 0.25$ and (b) $BV/TV = 0.46$. In each cycle plateau load was held constant for 200 s and strain recovery was measured for another 600 s. The load or stress levels in each of the loading cycle I, II, III, IV, V, and VI correspond to the static strains of 0.2%, 0.4%, 0.6%, 0.8%, 1.0%, and 1.5%, respectively.

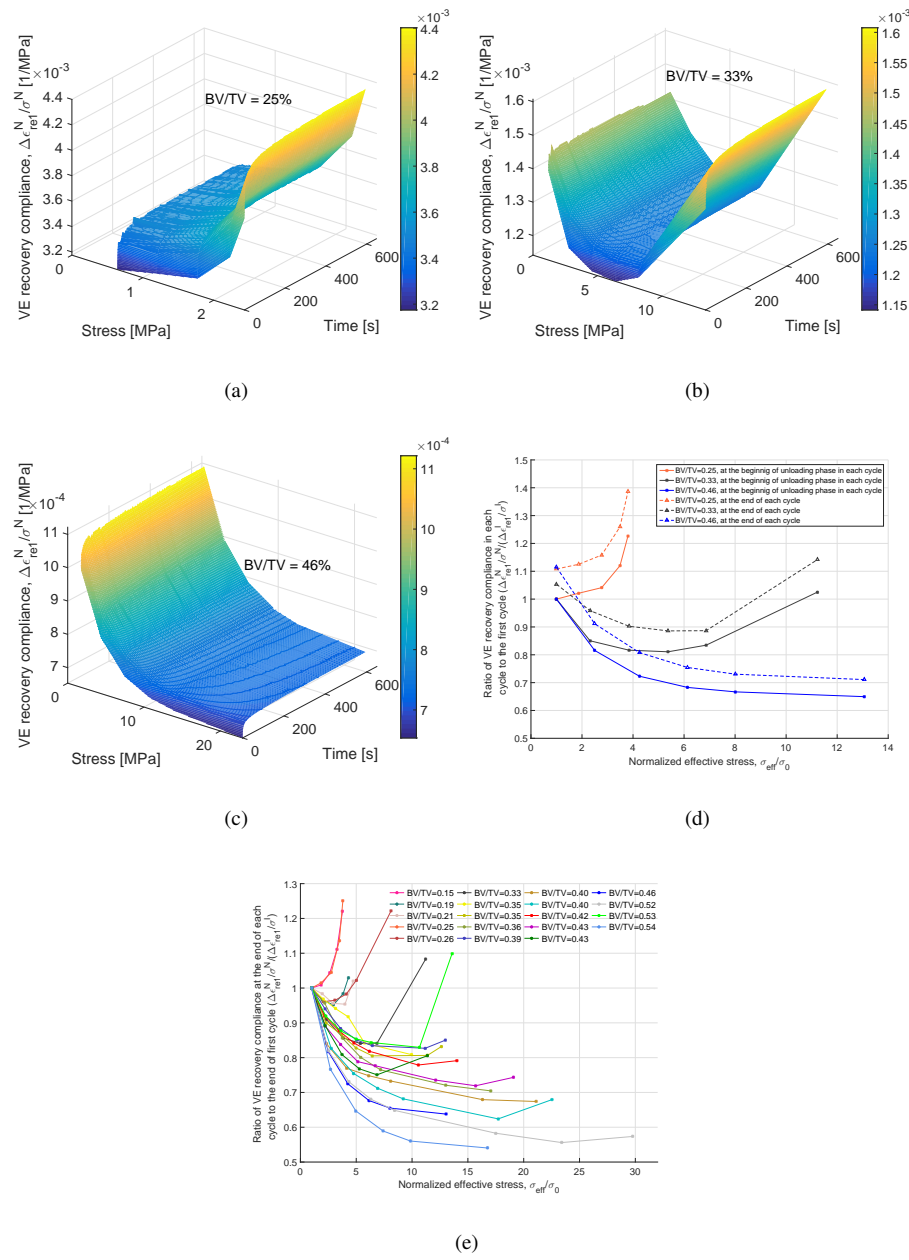
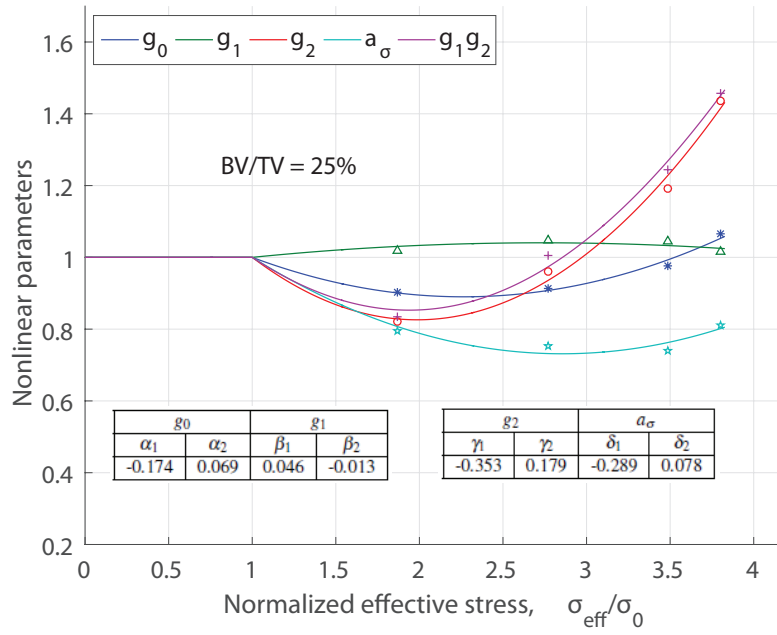
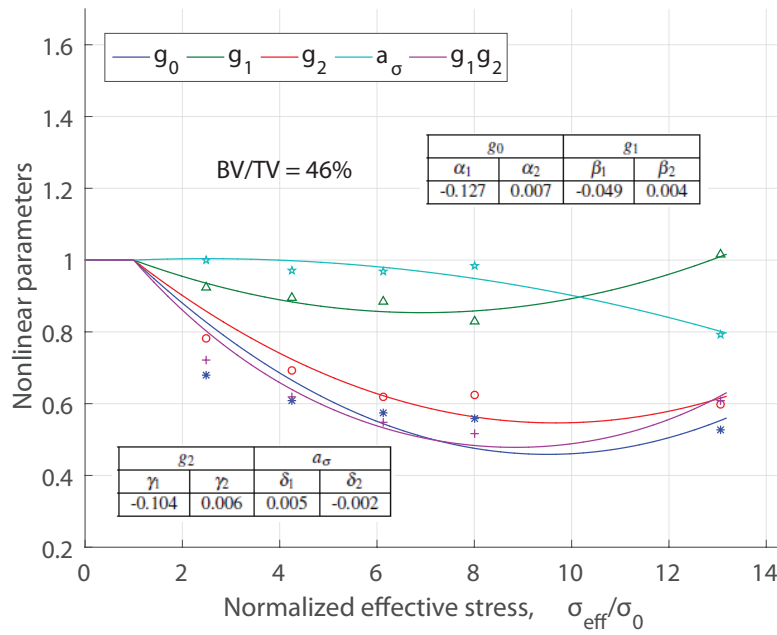


Fig. 4 Experimental viscoelastic recovery compliance with the time and stress for samples: (a) S25 (BV/TV = 0.25), (b) S33 (BV/TV = 0.33), and (c) S46 (BV/TV = 0.46); (d) the ratio between the viscoelastic recovery compliance and the respective instantaneous compliance for each of the three samples plotted against normalized effective stress, and (e) the ratio of viscoelastic recovery compliance at the end of each cycle to the respective value at the end of first cycle plotted against normalized effective stress for all 19 samples. Purely recoverable response was obtained from $\Delta \epsilon_{re1}^N$ in each loading cycle.



(a)



(b)

Fig. 5 Nonlinear viscoelastic parameters, g_0 , g_1 , g_2 and a_σ , expressed as second order polynomial functions of effective stress (Eqs. 19 - 22) are plotted against normalized effective stress for two samples with (a) BV/TV = 0.25 and (b) BV/TV = 0.46.

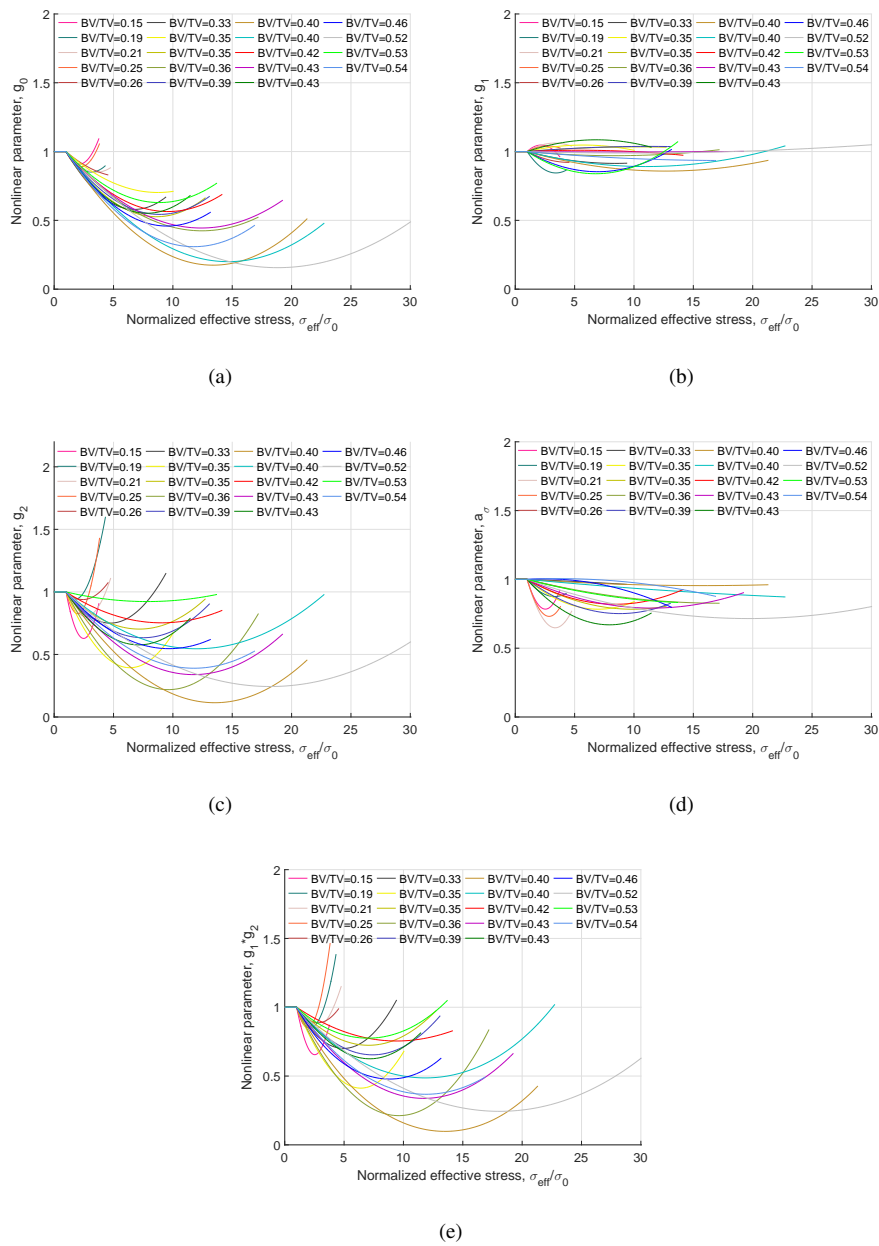
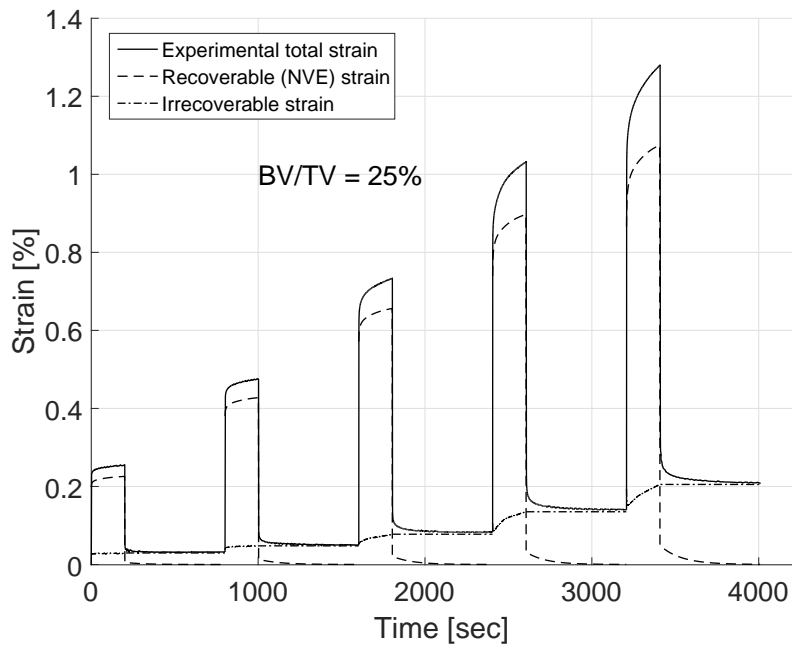
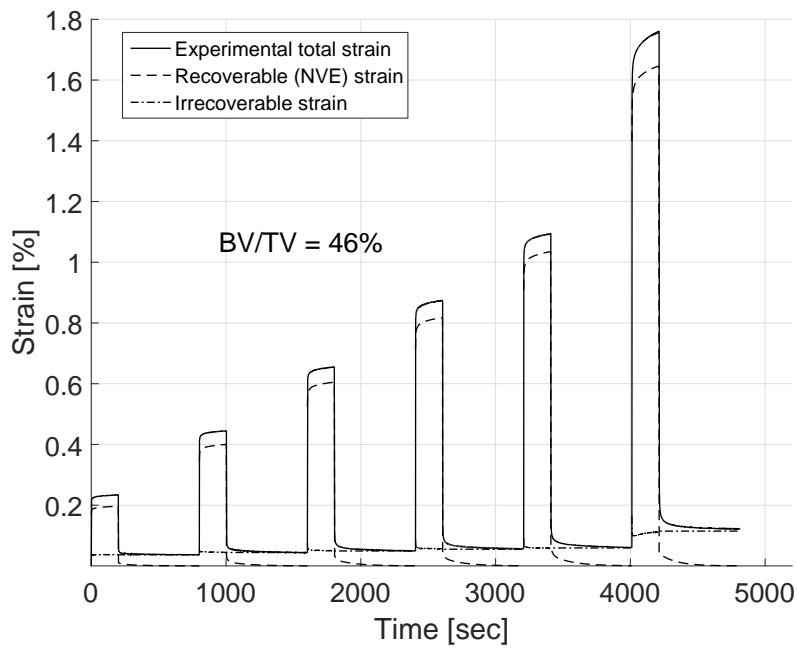


Fig. 6 Nonlinear VE parameters, expressed as second order polynomial functions of effective stress, for all 19 samples are plotted against normalized stress, (a) parameter g_0 , (b) parameter g_1 , (c) parameter g_2 , (d) parameter a_σ , and (e) product of the parameters g_1 and g_2 .

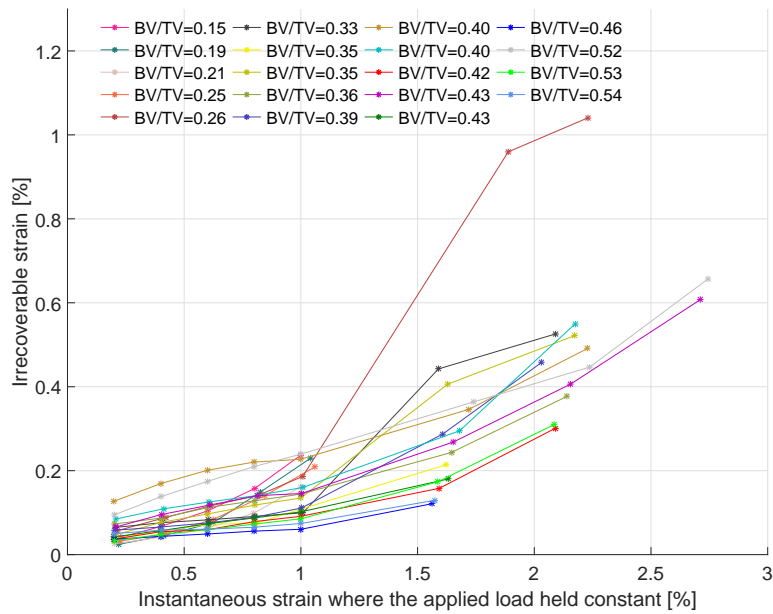


(a)

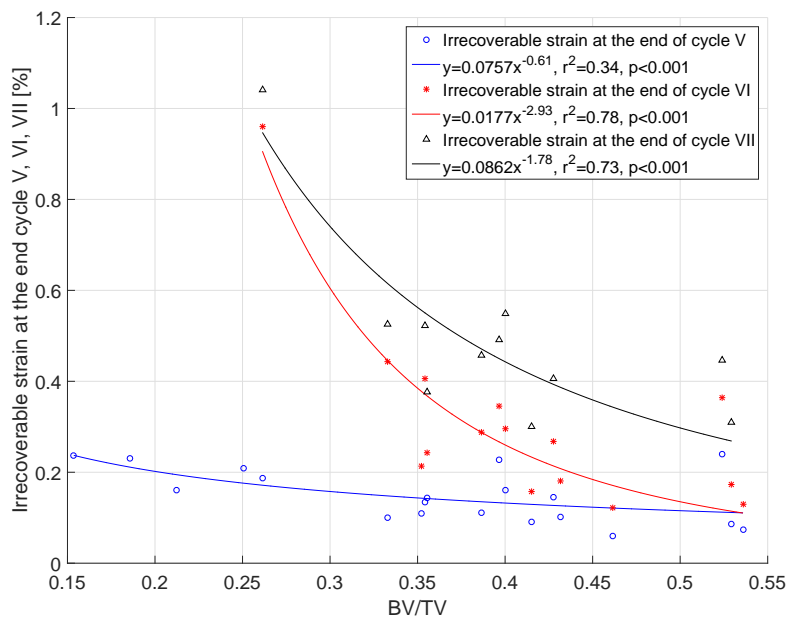


(b)

Fig. 7 The pure viscoelastic and the irrecoverable strain responses are plotted along with the total creep strain response for two typical samples S25 and S46, (a) $BV/TV = 0.25$ and (b) $BV/TV = 0.46$, respectively.



(a)



(b)

Fig. 8 (a) Irrecoverable strains at the end of each loading cycle in each sample with the applied static strain (where plateau force was held constant during creep-recovery test), (b) irrecoverable strains in cycle V, VI, VII corresponding to static strains of 1.0%, 1.5% and 2.0% are plotted against BV/TV of all samples.